tube for in vitro and in vivo experiments, respectively. After hydration, the dispersion was sonicated for 5 min in a bath sonicator to form liposomes and sterilized by filtration with a 0.45 μm filter (Nihon-Millipore, Tokyo, Japan).

Preparation of pCMV-OVA/liposome complexes. pCMV-OVA/liposome complexes for in vitro and in vivo experiments were prepared as described previously [20]. Briefly, equal volumes of pCMV-OVA and stock liposome solution were diluted with Hepes buffer or 5% dextrose in 1.5 ml Eppendorf tubes for in vitro and in vivo experiments, respectively. Then, pCMV-OVA solution was added rapidly to the surface of liposome solution using a micropipette (PIPETMAN, Gilson, Villier-le Bel, France) and the mixture was agitated rapidly by pumping it up and down twice in the pipet tip. For in vivo experiments, pCMV-OVA/liposome complexes were incubated at 4 °C for 12 h before use and pCMV-OVA (50 μg) was complexed with DC-Chol or Man liposome at a charge ratio of 1.0:2.3 (−:+) that is optimized charge for cell-selective gene transfection [28]. The mean particle sizes were measured by dynamic light scattering spectrophotometer (LS-900, Otsuka Electronics, Osaka, Japan).

Collection of macrophages. Mouse elicited peritoneal macrophages were cultured according to our previous report [29]. Briefly, peritoneal macrophages were obtained from C57BL/6 mice 4 days after intraperitoneal injection by 1 ml of 3% thioglycollate medium. Collected macrophages were plated on 96-well cluster dishes at a density of 1.3×10^5 cells/cm^2, respectively.

In vitro antigen-presenting assay. Antigen-presenting assay was performed after 72 h in cultured mouse elicited macrophages. Naked pCMV-OVA and that complexed with DC-Chol or Man liposomes at the weight ratio of 1:5 in Opti-MEM I were added to adherent macrophage in 96-well plate and incubated at 37 °C for 6 h. Then, medium was replaced with RPMI 1640 medium supplemented with 10% FBS and incubated for another 18 h. The cells were washed with ice-cold RPMI 1640 medium and fixed with 1% paraformaldehyde solution. Finally, 1×10^5 CD8OVA1.3 T cell hybridoma was added to each well and was incubated for 20 h. The activation of CD8OVA1.3 T cell hybridoma was evaluated by measuring IL-2 secreted to culture medium by commercial mouse IL-2 ELISA kit.

Quantification of OVA mRNA in CD11c$^+$ cells after intravenous injection by Real Time PCR. ICR mice were injected pDNA (50 μg) or that complex with liposomes twice at 30 min intervals. Spleens were harvested 6 h after second injection and spleen cells were suspended in ice-cold RPMI 1640 medium on ice. Positive selection of CD11c$^+$ cells was carried out by using magnetic cell sorting with auto MACS (Miltenyi Biotec, Auburn, CA, USA) following the manufacturer's instructions. Total RNA was isolated from CD11c$^+$ cells using MagExtractor MFX-2000 (TOYOBO, Osaka, Japan) and MagExtractor-RNA- following the manufacturer's instructions. Reverse transcription of mRNA was carried out using 1st strand cDNA synthesis kit as follows: total RNA was added to the oligo(dT) primer (0.8 μg/μl) solution and incubated at 42 °C for 60 min with program temperature control system PC-808 (ASTEC, Fukuoka, Japan). Real time PCR was performed using Lightcycler quick system 350S (Roche diagnostics, Indianapolis, IN, USA) with hybridization probes. Primer and hybridization probes for OVA cDNA were constructed as follows; primer, 4′-GCGTCTCTGAATTTAGGG-3′ (forward) and 4′-TACCCCTGATACTACAGTGC-3′ (reverse); hybridization probes, 4′-CTTCTGTATCAAGCACATCGCAACCAACG-3′-Fluorescein isothiocyanate (FITC) and LightCycler-Red640 (LCRed)-4′-CGTTCTCTTCTTTGGCAGATGTGTTTCCCC-3′. The PCR for detection of OVA gene was carried out in a 20 μl final volume containing: (1) 2 μl DNA Master Hybridization Probes 10× (DNA Master Hybridization Probes Kit); (2) 1.6 μl of 25 mM $MgCl_2$; (3) 1.5 μl of forward and reverse primers (final concentration 0.75 μM); (4) 1 μl of 2 μM FITC-labeled hybridization probes and 2 μl of 2 μM LCRed-labeled Probes (final concentration 0.2 and 0.4 μM, respectively); (5) 5.4 μl H_2O; and (6) 5 ml cDNA or pCMV-OVA solution. As for mouse β-actin cDNA measurement, samples were prepared following instruction manuals. After initial denaturation step at 95 °C for 10 min, temperature cycling was initiated. Each cycle consisted of denaturation at 95 °C for 10 s, hybridization at 60 °C for 15 s, and elongation at 72 °C for 10 s. The fluorescent signal was acquired at the end of the hybridization step (F2/F1 channels). A total of 45 cycles were performed. The mRNA copy numbers were calculated for each sample from the standard curve by the instrument software ("Arithmetic Fit Point analysis" for the Lightcycler). Results were expressed in relative copy numbers calculated relative to β-actin mRNA (copy number of OVA mRNA/copy number of β-actin mRNA).

Collection of dendritic cells and antigen presentation assay after intravenous administration. C57BL/6 mice were immunized with pCMV-OVA or that complexed with DC-Chol or Man liposomes by intravenous administration. At indicated time period, mice were sacrificed and spleens were harvested. The spleen cells were suspended in ice-cold RPMI 1640 medium on ice. Positive selection of CD11c$^+$ cells was carried out by using magnetic cell sorting with auto MACS (Miltenyi Biotec, Auburn, CA, USA). The cell suspension was incubated with anti-CD11c$^+$ monoclonal antibody (N418) labeled magnetic beads. Positively collected cells with auto MACS were suspended in RPMI 1640 medium supplemented with 10% FBS. CD11c$^+$ cells were placed in 96-well plate at various number and co-cultured with 1×10^5 cells of CD8OVA1.3 T cell hybridoma for 20 h. Activation of CD8OVA1.3 T cell hybridoma was evaluated by measuring IL-2 secreted to culture medium by commercial IL-2 ELISA kit.

Lymphocyte proliferation assay after intravenous administration. C57/BL6 mice were immunized with naked pCMV-OVA or that complexed with DC-Chol or Man liposomes by intravenous administration 3 times at 2 weeks interval. Four weeks after last immunization, spleens of each group were harvested and suspended in ice-cold RPMI 1640 medium. After 3-times wash, spleen cells were suspended in RPMI 1640 medium supplemented with 10% FBS. Spleen cells (5×10^5 cells) were placed in 96-well plate and incubated for 72 h at 37 °C in the presence or absence of OVA (100 μg). Then spleen cells were incubated for another 6 h in 10% AlamarBlue containing RPMI 1640 supplemented with 10% FBS. Proliferation was evaluated by measuring absorbance (Abs) at 570 and 590 nm and calculated from equation as follows:

(i) Percentage of reduction of AlamarBlue = (Abs (570 nm) − Abs (590 nm) × A) × 100.
(ii) $A = Abs_{t=0}$ (570 nm)/$Abs_{t=0}$ (590 nm).
(iii) Proliferation index = Percentage of reduction (OVA (+))/ Percentage of reduction (OVA (−)).

Results represent means of five separate spleen cell suspensions.

OVA-specific cytokine secretion from spleen cells. C57BL/6 mice were immunized with naked pCMV-OVA or that complexed with DC-Chol or Man liposomes by intravenous administration three times at intervals of 2 weeks. Four weeks after the last immunization, the spleens of each group were harvested and suspended in ice-cold RPMI 1640 medium. After washing three times, spleen cells were suspended in RPMI 1640 medium supplemented with 10% FBS. Spleen cells (5×10^5 cells) were placed in 96-well plates and incubated for 72 h at 37 °C in the presence or absence of OVA (100 μg). IFN-γ and IL-4 in the culture medium were measured by the commercial IFN-γ and IL-4 ELISA kit, respectively. Results represent means of five separate spleen cell suspensions.

Evaluation of cytokines in serum after intravenous administration of pDNA/liposome complexes. C57BL/6 mice were immunized by intravenous administration of naked pCMV-OVA or that complexed with DC-Chol or Man liposomes. Serum was collected from tail vein at predetermined time-periods and the concentrations of TNF-α, IL-12 (p70), and IFN-γ were measured by commercial ELISA kits.

Statistical analysis. Statistical comparisons were performed by Student's *t* test for two groups and one-way ANOVA for multiple groups. A value of $P < 0.05$ was considered to be indicative of statistical significance.

Results

Particle size analysis of pCMV-OVA/liposome complexes

pCMV-OVA complexed with Man liposomes or DC-Chol liposomes was prepared in 5% dextrose. The mean particle size is important for effective in vivo cell-selective gene transfection [13], so that the mean particle sizes were evaluated. The mean particle sizes of constructed pCMV-OVA complexed with Man liposomes and DC-Chol liposomes were confirmed to be 182.3 ± 7.4 ($n = 3$) and 175.8 ± 5.2 ($n = 3$) nm, respectively. These values are comparable with our previous results obtained with pCMV-Luc complexed with cationic liposomes that produced APC-selective gene transfection [20].

Antigen presentation in cultured mouse peritoneal macrophages

The expressed antigen in APCs can be subsequently processed and presented as peptide epitopes on the MHC class I molecules; consequently, antigen epitope-specific $CD8^+$ T cells are stimulated. Therefore, the antigen presentation was evaluated using cultured macrophages. As shown in Fig. 1, the Man liposome/pCMV-OVA complex induces secretion of IL-2 from a CD8OVA1.3 T cell hybridoma more strongly than naked pCMV-OVA and that complexed with DC-Chol liposomes, indicating that the Man liposome/pCMV-OVA complex produces more efficient antigen epitope presentation on the MHC class I complex than cationic liposomes.

OVA mRNA expression on $CD11c^+$ cells in the spleen after intravenous administration

To evaluate OVA gene expression on $CD11c^+$ cells after intravenous administration, total RNA was extracted from $CD11c^+$ cells in the spleen after intravenous administration of naked pCMV-OVA and that complex with Man or DC-Chol liposome and mRNA expression was evaluated by 2-step quantitative RT-PCR. Relative copy number of mRNA of OVA in Man liposome/pCMV-OVA injected group was the highest of all (Fig. 2). This result shows that Man liposome/pCMV-OVA enhance gene expression on $CD11c^+$ cells.

Antigen presentation on MHC class I $CD11c^+$ cells in the spleen after intravenous administration

To evaluate the antigen presentation under in vivo conditions, $CD11c^+$ cells in the spleen were separated after intravenous administration of naked pCMV-OVA and that complexed with Man and DC-Chol liposome and co-cultured with a CD8OVA1.3 T cell hybridoma. The IL-2 release by the Man liposome/pCMV-OVA complex was the highest of all (Fig. 3), suggesting that targeted delivery of DNA vaccine via the intravenous

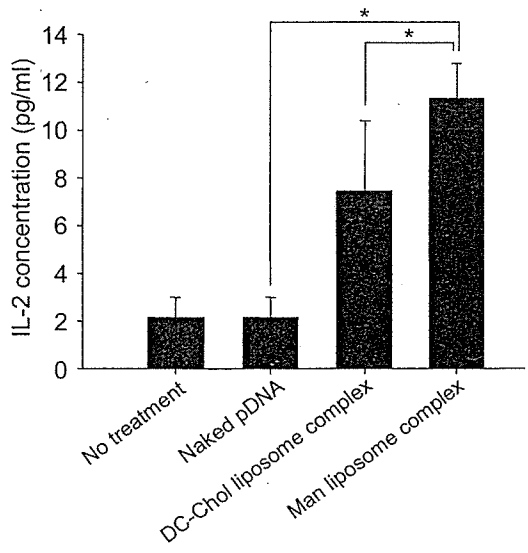

Fig. 1. Antigen presentation on MHC class I molecules in elicited mouse peritoneal macrophages after transfection with naked pCMV-OVA and that complexed with DC-Chol or Man liposomes. OVA peptide presentation was evaluated by IL-2 secretion from a CD8OVA1.3 T cell hybridoma during co-culture for 20 h with fixed macrophages. Each value represents mean + SD of five experiments. Statistical analysis was performed (*$P < 0.05$).

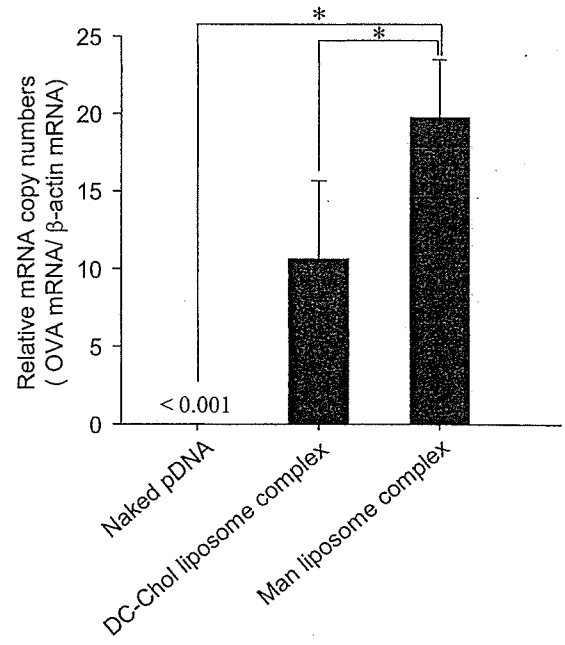

Fig. 2. Relative mRNA number of OVA gene in splenic $CD11c^+$ cells after intravenous administration of naked pCMV-OVA and that complexed with DC-Chol or Man liposomes. Each value shows the mean of relative copy number of OVA mRNA/β-actin mRNA value + SD of three experiments. Statistical analysis was performed (*$P < 0.05$).

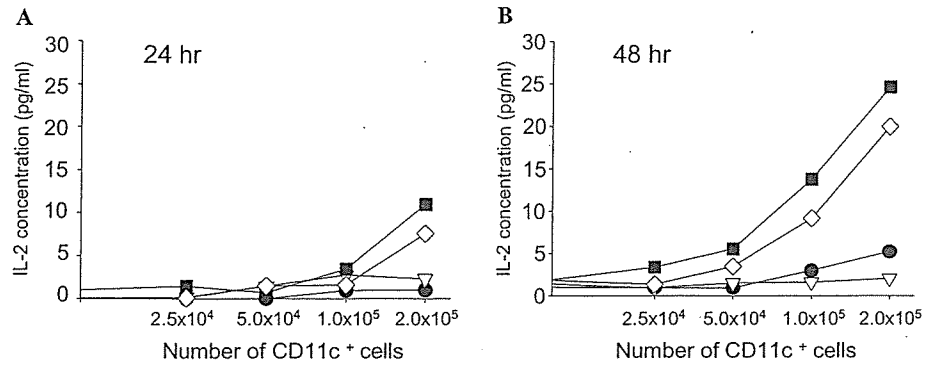

Fig. 3. Antigen presentation on MHC class I molecules in splenic CD11c$^+$ cells after intravenous administration of naked pCMV-OVA (▽) and that complexed with DC-Chol (◇) or Man (■) liposomes. (●) represents the no treatment group. OVA peptide presentation on MHC class I molecules in CD11c$^+$ cells was determined at 24 (A) and 48 (B) h with a CD8OVA1.3 T cell hybridoma. Each value represents the mean of pentapricated assay using a single pool of spleen cell suspension from 5 mice in each group.

route leads to CD8 T cell activation through enhancement of antigen epitope presentation on MHC class I molecules under in vivo conditions.

Induction of proinflammatory cytokine production after intravenous administration

The effect of liposome/pCMV-OVA complex injections on cytokine release was assessed by monitoring the cytokine levels in serum. Fig. 4 shows the time-course of TNF-α, IL-12, and IFN-γ concentrations in serum. After intravenous administration of naked pCMV-OVA, no cytokine release was detected. However, cytokine release was observed after intravenous administration of pCMV-OVA complexed with liposomes. The highest concentration of TNF-α, IL-12, and IFN-γ was observed at 3, 6, and 6 h, respectively. These observations regarding the cytokine release profiles by pDNA that complexed with cationic liposomes are in good agreement with other reports [30,31]. After intravenous administration of Man liposome/pCMV-OVA complex, a significantly higher induction of TNF-α, IL-12, and IFN-γ was observed, suggesting the higher uptake of pCMV-OVA to APCs by Man liposomes. Also, this observation is supported by our previous results showing that pCMV-Luc complexed with Man liposome could selectively transfect the luciferase, which is an encoded model gene, in APCs via mannose receptor-mediated endocytosis after intravenous administration [20].

Antigen (OVA)-specific proliferation of spleen cells and cytokine release after intravenous administration

To analyze the antigen-specific proliferation of spleen cells and cytokine release by spleen cells from immunized mice, suspensions of spleen cells were incubated in cultured medium containing OVA. The spleen cells from mice immunized with Man liposome/pCMV-OVA complex exhibited a higher proliferation response than those with naked pCMV-OVA and that complexed with DC-Chol liposomes (Fig. 5).

Spleen cells from mice immunized with Man liposome/pCMV-OVA complex produced the highest IFN-γ

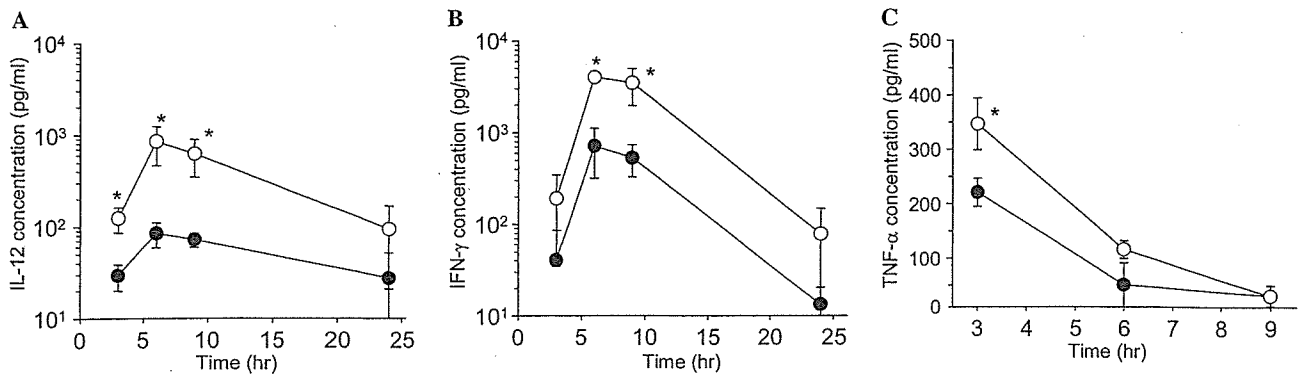

Fig. 4. Cytokine release profiles in serum after intravenous administration of pCMV-OVA complexed with DC-Chol (●) or Man (○) liposomes. IL-12 (A), IFN-γ (B), and TNF-α (C) in serum were determined by ELISA. Each value represents the mean ± SD of four experiments. Statistical analysis was performed (*$P < 0.05$).

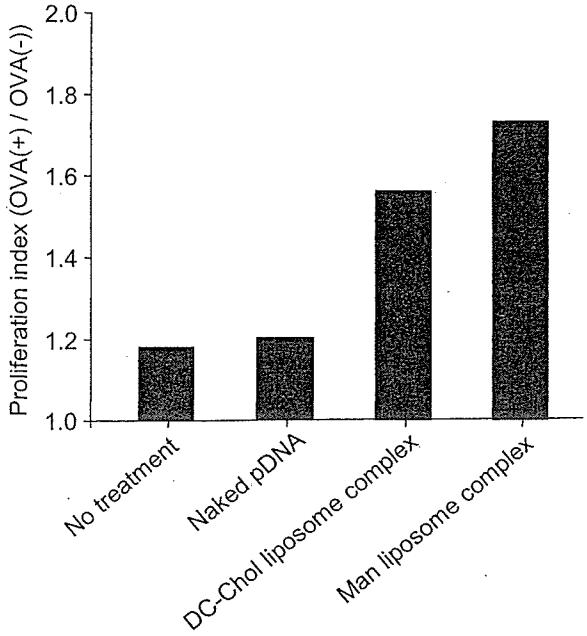

Fig. 5. Antigen (OVA)-specific proliferation response of spleen cells from mice immunized with naked pCMV-OVA and that complexed with DC-Chol or Man liposomes. After immunization by intravenous administration, spleen cells were cultured and stimulated with 100 μg OVA. Proliferation of spleen cells was evaluated by AlamarBlue. Each value represents mean of pentapricated assay using a single pool of spleen cell suspension from 5 mice in each group.

secretion of all (Fig. 6). In contrast, no IL-4 was detected in cultured medium of spleen cells in any of the experiments (data not shown).

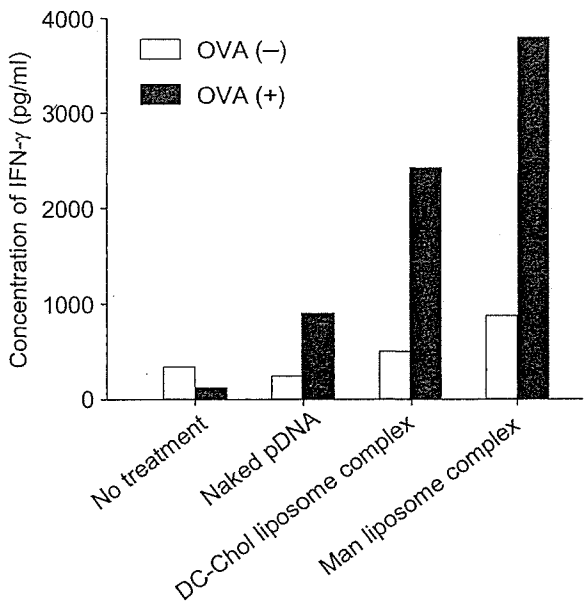

Fig. 6. Antigen-specific IFN-γ secretion by spleen cells from mice immunized with naked pCMV-OVA and that complexed with DC-Chol or Man liposomes. After immunization by intravenous administration, spleen cells were cultured in the absence (□) or presence (■) of 100 μg OVA. IFN-γ in the culture medium was evaluated by ELISA. Each value represents the mean of pentapricated assay using a single pool of spleen cell suspension from 5 mice in each group.

Discussion

This manuscript summarizes our initial efforts to investigate whether Man liposomes are able to act as potent carriers of DNA vaccine. Although topical application, intradermal, subcutaneous, and intramuscular injection of naked pDNA led to potent DNA vaccination in mice, leakage of pDNA from the injection site, trauma at the injection site, and limitations on the injection volume and/or dose are problems. In the present study, we selected the intravenous route for DNA vaccine immunization because it has many advantages compared with topical administration, including (i) firmness of administration, (ii) safety, (iii) relatively low restriction on administration volume, and (iv) the relatively large number of APCs in the spleen. In actual fact, an enhanced mRNA expression of OVA and MHC class I antigen presentation on APCs and an induced Th-1 polarized T cell response were observed after intravenous administration of the Man liposome/pCMV-OVA complex, suggesting that targeted delivery of pDNA to APCs offered an effective approach to DNA vaccine therapy.

DC maturation is crucial in the induction of an immune response in DNA vaccination [5]. In some animal models, it has been reported that pDNA itself possesses adjuvant properties determined by the presence of immunostimulatory sequences within the DNA vector backbone. To date, non-methylated, palindromic DNA-sequences containing CpG-oligonucleotides have been shown to activate dendritic cells, macrophages, monocytes, NK-cells, and B-cells, subsequently leading these cells to secrete proinflammatory cytokines, including TNF-α, IL-1, IL-6, and IL-12 [32,33]. These cytokines, especially IL-12, serve as strong adjuvants for the forward differentiation of helper T cells to type 1 helper T cell (Th1), which have been reported to play a pivotal role in the activation of the CTL response [32,34]. As shown in Fig. 4, the Man liposome/pCMV-OVA complex produces a stronger induction of IL-12, IFN-γ, and TNF-α than the unmodified liposome complex. Several investigators, including ourselves, have already reported that Kupffer cells, splenic macrophages, and DCs play a crucial role in this cytokine release [30,31]. Thus, this observation supports our previous results showing that the Man liposome/pDNA complex can be efficiently transfected to APCs after intravenous administration [20]. Also, such enhancement of Th1 cytokine secretion led us to surmise that the DNA vaccine potency is enhanced by biasing helper T cells towards differentiation to Th1 cells when DNA vaccine is administered with Man liposomes, indicating the usefulness of Man liposomes as a DNA vaccine carrier. In fact, spleen cells from mice immunized with the Man liposome/pCMV-OVA complex following intravenous administration induced the splenic T cell proliferation response strongly and led to the highest IFN-γ secretion, while there was no IL-4

secretion after stimulation with OVA (Figs. 5 and 6). These results suggest that facilitated differentiation to Th1 cells resulted from the administration of pDNA complexed with Man liposomes. Thus, targeted delivery of DNA vaccine to APCs is an effective approach for enhancing the potency of DNA vaccination therapy.

To accomplish efficient DNA vaccine therapy without adverse effect, reduction of gene expression on non-APCs is considered to be important because transfected non-APCs can be target of evoked CTL and that may result in organ failure. Man liposome/pDNA has potency to enhance gene expression on mannose receptor-expressing non-APC, i.e., vascular endothelial cells. However, accumulation of Man liposome/pDNA complex to these cells seems to be limited because our previous biodistribution study demonstrated that Man liposome/^{32}P-labeled pDNA complex showed rapid accumulation in the liver non-parenchymal cells [35], implying that gene expression on these cells might to be low and diminish before induction of CTL response. As for intravenous injection of cationic liposome/pDNA complexes, on the other hand, the highest gene expression was observed in the lung [20,36,37] and this seems to have a much impact on adverse effect.

In the present study, no measurable CTL response was observed (data not shown). Our previous studies using pCMV-Luc as a model gene showed that the luciferase expression in the liver and spleen after intravenous injection of the Man liposome/pCMV-Luc complex reached a maximum at 6 h and then fell within 24 h [35]. However, it has been reported that priming of naive T cells occurred in the T cell region by APCs in lymphoid tissue, including spleen, and priming efficacy is correlated with the duration of antigenic presentation [38]. In this context, prolonged gene expression to APCs by Man liposomes might be an important issue for efficient vaccination; therefore, further studies are needed to obtain effective CTL activity and this may include (i) stabilizing the complex, (ii) designing a pDNA construct, and (iii) altering the administration route. In conclusion, the present study has demonstrated that Man liposomes enhance gene expression of antigen and MHC class I antigen presentation on APCs and Th1 T cell response. However, a higher immunogenicity needs to be attained by modifying this system. These findings may indicate that targeted delivery of DNA vaccine by Man liposomes is a potent vaccination method for DNA vaccine therapy. Hence, the obtained information will be of value for the future use, design, and development of Man liposomes for in vivo applications involving DNA vaccine therapy.

Acknowledgments

We are grateful to Dr. C.V. Harding (Department of Pathology, Case Western Reserve University, Cleveland, OH, USA) and Dr. M.J. Bevan (Department of Immunology, University of Washington, Seattle, WA, USA) for providing us with CD8OVA1.3 T cell hybridoma and pAc-neo-OVA, respectively. This work was supported in part by Grants-in-Aid for Scientific Research from Ministry of Education, Culture, Sports, Science and Technology of Japan, and by Health and Labor Sciences Research Grants for Research on Hepatitis and BSE from the Ministry of Health, Labor and Welfare of Japan and by the 21st Century COE Program "Knowledge Information Infrastructure for Genome Science".

References

[1] J.B. Ulmer, J.J. Donnelly, S.E. Parker, G.H. Rhodes, P.L. Felgner, V.J. Dwarki, S.H. Gromkowski, R.R. Deck, C.M. DeWitt, A. Friedman, L.A. Hawe, K.R. Leander, D. Martinez, H.C. Perry, J.W. Shiver, D.L. Montgomery, M.A. Liu, Heterologous protection against influenza by injection of DNA encoding a viral protein, Science 259 (1993) 1745–1749.

[2] R. Schirmbeck, W. Bohm, K. Ando, F.V. Chisari, J. Reimann, Nucleic acid vaccination primes hepatitis B surface antigen specific cytotoxic T lymphocytes in non-responder mice, J. Virol. 69 (1995) 5929–5934.

[3] D.L. Doolan, M. Sedegah, R.C. Hedstrom, P. Hobart, Y. Charoenvit, S.L. Hoffman, Circumventing genetic restriction of protection against malaria with multigene DNA immunization: CD8$^+$ cell-, interferon γ-, and nitric oxide-dependent immunity, J. Exp. Med. 183 (1996) 1739–1946.

[4] T. Nishimura, M. Nakui, M. Sato, K. Iwakabe, H. Kitamura, M. Sekimoto, A. Ohta, T. Koda, S. Nishimura, The critical role of Th1-dominant immunity in tumor immunology, Cancer Chemother. Pharmacol. 46 (2000) S52–S61.

[5] O. Akbari, N. Panjwani, S. Garcia, R. Tascon, D. Lowrie, B. Stockinger, DNA vaccination: transfection and activation of dendritic cells as key events for immunity, J. Exp. Med. 189 (1999) 169–178.

[6] R.M. Steinman, The dendritic cell system and its role in immunogenicity, Annu. Rev. Immunol. 9 (1991) 271–296.

[7] J. Banchereau, R.M. Steinman, Dendritic cells and the control of immunity, Nature 392 (1998) 245–252.

[8] J.A. Wolff, R.W. Malone, P. Williams, W. Chong, G. Acsadi, A. Jani, P.L. Felgner, Direct gene transfer into mouse muscle in vivo, Science 247 (1990) 1465–1468.

[9] M.J. Roy, M.S. Wu, L.J. Barr, J.T. Fuller, L.G. Tussey, S. Speller, J. Culp, J.K. Burkholder, W.F. Swain, R.M. Dixon, G. Widera, R. Vessey, A. King, G. Ogg, A. Gallimore, J.R. Haynes, D. Heydenburg Fuller, Induction of antigen-specific CD8$^+$ T cells, T helper cells, and protective levels of antibody in humans by particle-mediated administration of a hepatitis B virus DNA vaccine, Vaccine 19 (2000) 764–778.

[10] S.A. Rosenberg, J.C. Yang, R.M. Sherry, P. Hwu, S.L. Topalian, D.J. Schwartzentruber, N.P. Restifo, L.R. Haworth, C.A. Seipp, L.J. Freezer, K.E. Morton, S.A. Mavroukakis, D.E. White, Inability to immunize patients with metastatic melanoma using plasmid DNA encoding the gp100 melanoma-melanocyte antigen, Hum. Gene Ther. 14 (2003) 709–714.

[11] L. Huang, S. Li, Liposomal gene delivery: a complex package, Nat. Biotechnol. 15 (1997) 620–621.

[12] M. Hashida, M. Nishikawa, F. Yamashita, Y. Takakura, Cell-specific delivery of genes with glycosylated carriers, Adv. Drug Deliv. Rev. 52 (2001) 187–196.

[13] S. Kawakami, F. Yamashita, K. Nishida, J. Nakamura, M. Hashida, Glycosylated cationic liposomes for cell-selective gene delivery, Crit. Rev. Ther. Drug Carrier Syst. 19 (2002) 171–190.

[14] G. Gregoriadis, R. Saffie, B. de Souza, Liposome-mediated DNA vaccination, FEBS Lett. 402 (1997) 107–110.

[15] L.S. Klavinskis, L. Gao, C. Barnfield, T. Lehner, S. Parker, Mucosal immunization with DNA-liposome complexes, Vaccine 15 (1997) 818–820.
[16] Y. Perrie, P.M. Frederik, G. Gregoriadis, Liposome-mediated DNA vaccination: the effect of vesicle composition, Vaccine 19 (2001) 3301–3310.
[17] N. Ishii, J. Fukushima, T. Kaneko, E. Okada, K. Tani, S.I. Tanaka, K. Hamajima, K.Q. Xin, S. Kawamoto, W. Koff, K. Nishioka, T. Yasuda, K. Okuda, Cationic liposomes are a strong adjuvant for a DNA vaccine of human immunodeficiency virus type 1, AIDS Res. Hum. Retroviruses 13 (1997) 1421–1428.
[18] M. Tanaka, Y. Kaneda, S. Fujii, T. Yamano, K. Hashimoto, S.K. Huang, D.S. Hoon, Induction of a systemic immune response by a polyvalent melanoma-associated antigen DNA vaccine for prevention and treatment of malignant melanoma, Mol. Ther. 5 (2002) 291–299.
[19] S. Toda, N. Ishii, E. Okada, K.I. Kusakabe, H. Arai, K. Hamajima, I. Gorai, K. Nishioka, K. Okuda, HIV-1-specific cell-mediated immune responses induced by DNA vaccination were enhanced by mannan-coated liposomes and inhibited by anti-interferon-γ antibody, Immunology 92 (1997) 111–117.
[20] S. Kawakami, A. Sato, M. Nishikawa, F. Yamashita, M. Hashida, Mannose receptor-mediated gene transfer into macrophages using novel mannosylated cationic liposomes, Gene Ther. 7 (2000) 292–299.
[21] S. Kawakami, J. Wong, A. Sato, Y. Hattori, F. Yamashita, M. Hashida, Biodistribution characteristics of mannosylated, fucosylated, and galactosylated liposomes in mice, Biochim. Biophys. Acta 1524 (2000) 258–265.
[22] H. Farhood, N. Serbina, L. Huang, The role of dioleoyl phosphatidylethanolamine in cationic liposome mediated gene transfer, Biochim. Biophys. Acta 1235 (1995) 289–295.
[23] S. Kawakami, A. Sato, M. Yamada, F. Yamashita, M. Hashida, The effect of lipid composition on receptor-mediated in vivo gene transfection using mannosylated cationic liposomes in mice, STP Pharma Sci. 11 (2001) 117–120.
[24] X. Gao, L. Huang, A novel cationic liposome reagent for efficient transfection of mammalian cells, Biochem. Biophys. Res. Commun. 179 (1991) 280–285.
[25] N.S. Potter, C.V. Harding, Neutrophils process exogenous bacteria via an alternate class I MHC processing pathway for presentation of peptides to T lymphocytes, J. Immunol. 167 (2001) 2538–2546.
[26] S. Kawakami, F. Yamashita, M. Nishikawa, Y. Takakura, M. Hashida, Asialoglycoprotein receptor-mediated gene transfer using novel galactosylated cationic liposomes, Biochem. Biophys. Res. Commun. 252 (1998) 78–83.
[27] Y.C. Lee, C.P. Stowell, M.J. Krantz, 2-Imino-2-methoxyethyl 1-thioglycosides: new reagents for attaching sugars to proteins, Biochemistry 15 (1976) 3956–3963.
[28] S. Kawakami, S. Fumoto, M. Nishikawa, F. Yamashita, M. Hashida, In vivo gene delivery to the liver using novel galactosylated cationic liposomes, Pharm. Res. 17 (2000) 306–313.
[29] T. Takagi, M. Hashiguchi, R.I. Mahato, H. Tokuda, Y. Takakura, M. Hashida, Involvement of specific mechanism in plasmid DNA uptake by mouse peritoneal macrophages, Biochem. Biophys. Res. Commun. 245 (1998) 729–733.
[30] D. Schattenberg, M. Schott, G. Reindl, T. Krueger, D. Tschoepe, J. Feldkamp, W.A. Scherbaum, J. Seissler, Response of human monocyte-derived dendritic cells to immunostimulatory DNA, Eur. J. Immunol. 30 (2000) 2824–2831.
[31] F. Sakurai, T. Terada, K. Yasuda, F. Yamashita, Y. Takakura, M. Hashida, The role of tissue macrophages in the induction of proinflammatory cytokine production following intravenous injection of lipoplexes, Gene Ther. 9 (2002) 1120–1126.
[32] T. Sparwasser, T. Miethke, G. Lipford, K. Borschert, H. Hacker, K. Heeg, H. Wagner, Bacterial DNA causes septic shock, Nature 386 (1997) 336–337.
[33] T. Sparwasser, E.S. Koch, R.M. Vabulas, K. Heeg, G.B. Lipford, J.W. Ellwart, H. Wagner, Bacterial DNA and immunostimulatory CpG oligonucleotides trigger maturation and activation of murine dendritic cells, Eur. J. Immunol. 28 (1998) 2045–2054.
[34] M.K. Gately, U. Gubler, M.J. Brunda, R.R. Nadeau, T.D. Anderson, J.M. Lipman, U. Sarmiento, Interleukin-12: a cytokine with therapeutic potential in oncology and infectious diseases, Ther. Immunol. 1 (1994) 187–196.
[35] M. Yamada, M. Nishikawa, S. Kawakami, Y. Hattori, T. Nakano, F. Yamashita, M. Hashida, Tissue and intrahepatic distribution and subcellular localization of a mannosylated cationic liposome/plasmid DNA complex after intravenous administration in mice, J. Control Release (in press).
[36] S. Li, M.A. Rizzo, S. Bhattacharya, L. Huang, Characterization of cationic lipid–protamine–DNA (LPD) complexes for intravenous gene delivery, Gene Ther. 5 (1998) 930–937.
[37] Y.K. Song, F. Liu, S. Chu, D. Liu, Characterization of cationic liposome-mediated gene transfer in vivo by intravenous administration, Hum. Gene Ther. 8 (1997) 1585–1594.
[38] R.M. Zinkernagel, S. Ehl, P. Aichele, S. Oehen, T. Kundig, H. Hengartner, Antigen localisation regulates immune responses in a dose- and time-dependent fashion: a geographical view of immune reactivity, Immunol. Rev. 156 (1997) 199–209.

doi:10.1016/j.ymthe.2004.07.015

ARTICLE

Enhanced Hepatocyte-Selective *in Vivo* Gene Expression by Stabilized Galactosylated Liposome/Plasmid DNA Complex Using Sodium Chloride for Complex Formation

Shintaro Fumoto, Shigeru Kawakami, Yoshitaka Ito, Kosuke Shigeta, Fumiyoshi Yamashita, and Mitsuru Hashida*

Department of Drug Delivery Research, Graduate School of Pharmaceutical Sciences, Kyoto University, Sakyo-ku, Kyoto 606-8501, Japan

**To whom correspondence and reprints requests should be addressed. Fax: +81 75 753 4575. E-mail: hashidam@pharm.kyoto-u.ac.jp.*

Available online 28 August 2004

In this study, we demonstrated that the presence of an essential amount of sodium chloride (NaCl) during the formation of cationic liposome/plasmid DNA complexes (lipoplexes) stabilizes the lipoplexes according to the surface charge regulation (SCR) theory. Fluorescence resonance energy transfer analysis revealed that cationic liposomes in an SCR lipoplex (5 and 10 mM NaCl solution in lipoplex) increased fusion. Also, aggregation of SCR lipoplexes was significantly delayed after exposure to saline (150 mM NaCl) as a model of physiological conditions. After intraportal administration, the hepatic transfection activity of galactosylated SCR lipoplexes (5 and 10 mM NaCl solution in lipoplex) was approximately 10- to 20-fold higher than that of galactosylated conventional lipoplexes in mice. The transfection activity in hepatocytes of galactosylated SCR lipoplexes was significantly higher than that of conventional lipoplexes, and preexposure to competitive asialoglycoprotein-receptor blocker significantly reduced the hepatic gene expression, suggesting that hepatocytes are responsible for high hepatic transgene expression of the galactosylated SCR lipoplexes. Pharmacokinetic studies both *in situ* and *in vivo* demonstrated a higher tissue binding affinity and a greater expanse of intrahepatic distribution by galactosylated SCR lipoplexes. Moreover, enhanced transfection activity of galactosylated SCR lipoplexes was observed in HepG2 cells, and investigation of confocal microscopic images showed that the release of plasmid DNA in the cell was markedly accelerated. These characteristics partly explain the mechanism of enhanced *in vivo* transfection efficacy by galactosylated SCR lipoplexes. Hence, information in this study will be valuable for the future use, design, and development of ligand-modified lipoplexes for *in vivo* applications.

Key Words: gene therapy, cationic liposomes, targeting, plasmid DNA, hepatocytes

INTRODUCTION

Gene delivery to hepatocytes is of great therapeutic potential, since the cells are responsible for the synthesis of a wide variety of proteins that play important biological roles both inside and outside the liver. Despite the high transfection efficiency of viral vectors, safety concerns have been raised in clinical trials because of their highly toxic nature [1]. The use of nonviral vectors has attracted great interest for in vivo gene delivery because they are free of some of the risks inherent in these systems. Furthermore, the characteristics of nonviral vectors can be more easily modified than those of viral vectors. To achieve targeted gene delivery, a number of receptor-mediated gene delivery systems have been developed [2–5], including our carriers [6–10]. As far as in vivo selective gene delivery to hepatocytes is concerned, galactose has been shown to be a promising targeting ligand to hepatocytes (liver parenchymal cells) because the cells possess a large number of asialoglycoprotein receptors that recognize the galactose units on the oligosaccharide chains of glycoproteins or on the chemically synthesized galactosylated carriers [11]. Recently, we have developed several types of macromolecular [6,7] and particulate [9] gene carriers for hepatocyte-selective gene transfection in vivo. Among them, cationic liposomes containing cholesten-5-yloxy-*N*-(4-((1-imino-2-D-thiogalactosylethyl)amino)butyl) formamide (Gal-C4-Chol)[1] are one of the potential gene transfection carriers [8,9] that can be efficiently recognized by asialoglycoprotein receptors in hepatocytes. More recently, however, we have demon-

1525-0016/$30.00

doi:10.1016/j.ymthe.2004.07.015

strated that the penetration of the galactosylated liposome/pDNA complex (lipoplex) through the hepatic fenestrated endothelium to the parenchymal cells was greatly restricted in perfused rat liver [12]. Taking this into consideration, the stabilization and/or size reduction of galactosylated lipoplex is expected to improve the transfection efficiency *in vivo* due to greater accessibility to hepatocytes.

Although there are some current methodologies for stabilizing and/or reducing the size of nonviral carriers, each method has a disadvantage involving the transfection efficiency. For example, some reports have shown that sonication of lipoplexes reduces the diameter [13,14]; however, only 40% of pDNA in the optimized formulation is unbroken as the sum of relaxed and supercoiled forms after a 3-min sonication, and a marked reduction in the supercoiled form is observed even after a 1-min sonication [13]. The detergent dialysis method using PEGylated lipids also produces an average diameter of 70 nm; however, the surface modification of liposomes with PEG results in a reduced interaction with cells so that the system exhibits a low transfection potential [15]. For the rational design of hepatocyte-targeted gene carrier systems, the lipoplex needs to be stabilized and/or reduced in the size without losing the transfection activity.

Lipoplexes are often prepared in a nonionic solution due to their well-known tendency to aggregate out of solution as the salt concentration is increased [9,16,17]. Aggregation during lipoplex formation in ionic solution might be due to neutralization of the surface positive charge of the lipoplex intermediate by the associated counterion. Taking into account neutralization by counterion, we hypothesized that the presence of an essential amount of sodium chloride (NaCl) during lipoplex formation might regulate repulsion between cationic liposomes and fusion of cationic liposomes in the lipoplex would be accelerated by partial neutralization of the positive charge. Consequently, pDNA in the lipoplex could be largely covered by cationic lipids while retaining enough positive charge to prevent aggregate formation. Such types of lipoplex are expected to be more stable than the conventional lipoplex, which is prepared using a nonionic solution. To evaluate this hypothesis, we investigated the physicochemical properties and *in vivo* gene transfection efficacy of galactosylated "surface charge regulated" (SCR) lipoplex, prepared in the presence of an essential amount of NaCl during lipoplex formation, as a novel approach to stabilization. Also, the intrahepatic and intracellular dispositions of galactosylated SCR lipoplexes were examined to prove the mechanism of *in vivo* gene transfection.

RESULTS

Physicochemical Characteristics and Stability after Mixing Galactosylated SCR Lipoplexes with Saline

As shown in Fig. 1A, the particle size of the lipoplex was dependent on the concentration of NaCl in the lipoplex solution. When we increased the NaCl concentration in the lipoplex solution from 0 to 5 mM, the mean particle size of the lipoplexes decreased from 140 to 120 nm. At NaCl concentrations more than 5 mM, the particle size of the lipoplexes increased. These results indicate that the

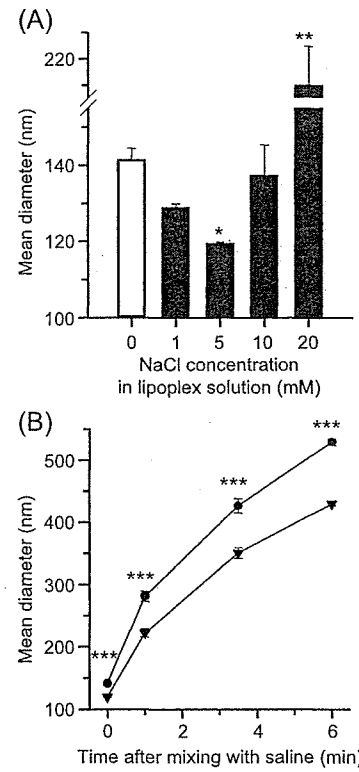

FIG. 1. (A) Difference in particle size of galactosylated lipoplexes. The particle size of galactosylated lipoplexes was measured by dynamic light scattering spectrophotometry. Each bar represents the mean diameter + SD of three experiments. Statistical comparisons with galactosylated conventional lipoplexes were performed using Dunnett's test at a significance level of 5 (*) and 1% (**). (B) Stability of galactosylated lipoplexes after mixing with saline as a model of physiological conditions. Each symbol represents the mean diameter ± SD of three experiments of galactosylated SCR lipoplexes (▼, 5 mM NaCl in lipoplex solution) or galactosylated conventional lipoplexes (●, 0 mM NaCl in lipoplex solution). Statistical comparisons were performed using an unpaired Student *t* test at each time point (***$P < 0.001$).

[1] Abbreviations used: pDNA, plasmid DNA; DOTMA, *N*-[1-(2,3-dioleyloxy)propyl]-*n,n,n*-trimethylammonium chloride; Chol, cholesterol; Gal-C4-Chol, cholesten-5-yloxy-*N*-(4-((1-imino-2-D-thiogalactosylethyl)amino)butyl)-formamide; lipoplex, cationic liposome/pDNA complex; SCR lipoplex, surface charge-regulated lipoplex; Gal-BSA, galactosylated bovine serum albumin; PC, parenchymal cells; NPC, nonparenchymal cells.

particle size of the lipoplex can be controlled by the NaCl concentration in the lipoplex solution. The mean diameter of galactosylated SCR lipoplexes (5 mM NaCl) did not change for 2 weeks at 4°C, suggesting that the SCR lipoplex was stable in size during storage (data not shown). To assess the stability of the SCR lipoplex under physiological conditions, we measured the particle size–time profile of the lipoplex after mixing the lipoplexes with saline (150 mM NaCl) solution (Fig. 1B). Galactosylated SCR lipoplexes (5 mM NaCl) significantly delayed particle size enlargement of the galactosylated conventional lipoplexes. In contrast, the particle size of the cationic liposomes remained unchanged after mixing with saline (data not shown).

Fluorescence Resonance Energy Transfer (FRET) Analysis of SCR Lipoplex

We performed FRET analysis to evaluate further the formation of galactosylated SCR lipoplexes (Fig. 2). We evaluated the FRET effect using the peak ratio of nitrobenzoxadiazol (NBD) and rhodamine (Rh). First, we measured the changes in liposome–liposome interaction of the SCR lipoplexes using NBD- and Rh-labeled liposomes (Fig. 2A). We observed distinct energy transfer from NBD (emission 534 nm) to Rh (emission 590 nm) in galactosylated SCR lipoplexes (5 and 10 mM NaCl) and the NBD/Rh fluorescence intensity ratio (F534/F590) was 2.12 ± 0.18, 1.55 ± 0.13, and 1.39 ± 0.085 ($n = 3$) for 0, 5, and 10 mM NaCl solution, respectively, suggesting that each cationic liposome in the galactosylated SCR lipoplexes (5 and 10 mM NaCl ($P < 0.01$)) had significantly easier access to the others than the galactosylated conventional lipoplexes (0 mM NaCl).

It has been reported that cationic liposomes in the lipoplex are fused to one another [17–19]. To evaluate the fusion of cationic liposomes in the galactosylated SCR lipoplex, we mixed NBD–Rh double-labeled liposomes with unlabeled liposomes and measured the fusion of each of the cationic liposomes during lipoplex formation (Fig. 2B). Although the fluorescence intensities of NBD and Rh in liposomes before lipoplex formation were almost the same level (F534/F590 = 1.15), the fluorescence intensities of NBD in each of the galactosylated lipoplexes were greatly increased, suggesting the fusion of each of the cationic liposomes in these lipoplexes. The NBD/Rh ratio (F534/F590) was 2.04 ± 0.09, 2.26 ± 0.05, and 2.39 ± 0.02 for 0, 5, and 10 mM NaCl solution, suggesting that the cationic liposomes in the galactosylated SCR lipoplex are greatly fused compared with conventional lipoplex ($P < 0.01$ ($n = 3$)).

We evaluated the pDNA–cationic liposome interaction using PicoGreen-labeled pDNA and Rh-labeled liposomes (Fig. 2C). The fluorescence intensities at the PicoGreen emission wavelength (520 nm) were drastically increased by the galactosylated SCR lipoplexes, while no significant changes were observed at the Rh emission wavelength (590 nm). The PicoGreen/Rh ratio (F520/F590) was 0.66 ± 0.04, 0.88 ± 0.03, and 0.88 ± 0.02 for 0, 5, and 10 mM

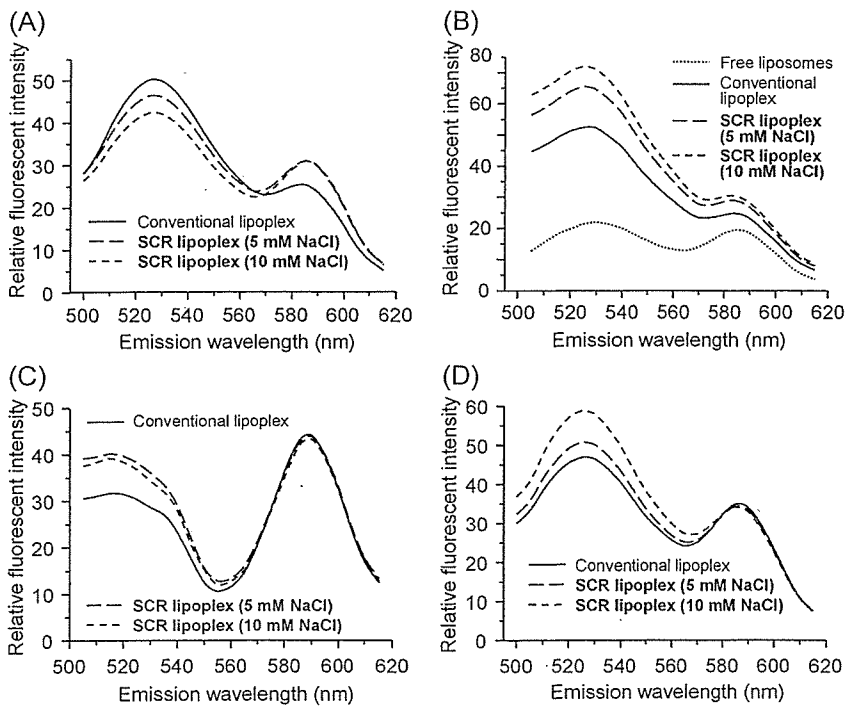

FIG. 2. FRET analysis of galactosylated SCR lipoplex formation. (A) Liposome–liposome interaction. NBD–liposomes and Rh–liposomes were mixed at a ratio of 1:1 prior to lipoplex formation. Thirty minutes after pDNA was mixed with a mixture of NBD- and Rh-labeled liposomes, the fluorescence intensity spectra were measured at an excitation wavelength of 460 nm. (B) Fusion among liposomes in the lipoplexes. NBD and Rh double-labeled liposomes were mixed with unlabeled liposomes at a ratio of 1:4 prior to lipoplex formation. Thirty minutes after lipoplex formation, the fluorescence intensity spectra were measured at an excitation wavelength of 460 nm. (C) pDNA–liposome interaction. Thirty minutes after Rh-labeled liposomes were mixed with PicoGreen-labeled pDNA, the fluorescence intensity spectra were measured at an excitation wavelength of 480 nm. (D) Spectral change after the galactosylated lipoplexes were mixed with saline. NBD–lipoplexes and Rh–lipoplexes were separately prepared. Thirty minutes after lipoplex formation, NBD- and Rh-labeled lipoplexes were mixed at a volume ratio of 1:1. One minute after the galactosylated lipoplexes were mixed with saline at a volume ratio of 3:17, the fluorescence intensity spectra were measured at an excitation wavelength of 460 nm.

doi:10.1016/j.ymthe.2004.07.015

NaCl solution, respectively, suggesting that the pDNA–liposome interaction with the galactosylated SCR lipoplexes was significantly weaker than that with conventional lipoplexes ($P < 0.01$ ($n = 3$)).

To support the stabilization effect of galactosylated SCR lipoplex after mixing with saline as shown in Fig. 1B, we performed FRET analysis following mixing with saline using NBD-labeled lipoplex and Rh-labeled lipoplex (Fig. 2D). We observed marked FRET in galactosylated conventional lipoplexes after mixing them with saline, while the FRET in galactosylated SCR lipoplexes was less than that in galactosylated conventional lipoplexes. The NBD/Rh ratio (F534/F590) was 1.32 ± 0.02, 1.41 ± 0.02, and 1.64 ± 0.02 for 0, 5, and 10 mM NaCl solution, respectively, suggesting that galactosylated SCR lipoplexes can significantly prevent aggregation after exposure to saline ($P < 0.01$ ($n = 3$)). Similar results were obtained when lipoplexes were diluted with phosphate-buffered saline (PBS) containing 10% fetal bovine serum (3.68 ± 0.21, 5.12 ± 0.23, and 5.51 ± 0.70 for 0, 5, and 10 mM NaCl solution, respectively ($n = 3$)), supporting the notion that SCR lipoplexes (5 and 10 mM NaCl) were more stable than conventional lipoplexes under physiological conditions.

Enhanced Hepatocyte-Selective *in Vivo* Gene Expression and Intrahepatic Distribution of Galactosylated SCR Lipoplex

Fig. 3 shows the hepatic transfection activity of galactosylated SCR lipoplexes after intraportal administration in mice. The hepatic transfection activity of galactosylated SCR lipoplexes was markedly enhanced and ranged from 2- to 20-fold higher than that of the conventional lipoplexes; in particular, SCR lipoplexes at 5 mM NaCl solution exhibited the highest transfection activity (Fig. 3A). To assess organ selectivity, we compared the luciferase activities in the liver with those in the lung, which exhibited secondary high expression by lipoplex [9]. The liver/lung gene expression ratio (liver selectivity index) was 5.4 and 42 for galactosylated conventional and SCR lipoplexes, indicating that the liver selectivity of the galactosylated SCR lipoplexes was much higher (Fig. 3B). At doses ranging from 15 to 30 μg, we also observed an enhanced hepatic gene expression by galactosylated SCR lipoplexes (Fig. 3C). Furthermore, galactosylated SCR lipoplexes (5 mM NaCl) maintained significantly higher transfection activity for 6, 12, and 24 h than the galactosylated conventional lipoplexes (Fig. 3D).

To evaluate the hepatocyte selectivity in liver cells, we performed inhibition experiments using galactosylated bovine serum albumin (Gal-BSA) and separation of the hepatocytes (the target cells) from other liver cells (liver nonparenchymal cells) (Fig. 4). When we administered an excess amount of Gal-BSA, which is a ligand of the asialoglycoprotein receptor, intravenously 5 min prior to the intraportal administration of galactosylated SCR lipoplexes, the gene expression in the liver was significantly inhibited by the preadministration of Gal-BSA, suggesting involvement of receptor-mediated endocytosis (Fig. 4A). Furthermore, the transgene expression in hepatocytes of galactosylated SCR lipoplexes was significantly higher than that of conventional lipoplexes (Fig. 4B) and the hepatocytes/liver nonparenchymal cells transgene expression ratio of galactosylated SCR lipoplexes (ratio = 3.84) was higher than that of conventional lipoplexes (ratio = 1.86). These results suggest that hepatocytes are responsible for high hepatic transgene expression of the galactosylated SCR lipoplexes.

To confirm the hepatic distribution of the lipoplexes, we labeled pDNA fluorescently and then evaluated the intrahepatic distribution by observation of frozen liver sections. As shown in Fig. 5, the fluorescence intensity of the galactosylated SCR lipoplexes was more marked and extensive than that of the galactosylated conventional lipoplexes. We obtained similar results using galactosylated lipoplexes containing NBD-labeled liposomes (data not shown). The *in vivo* intrahepatic distribution results partly support the enhanced hepatic *in vivo* transfection activity of the galactosylated SCR lipoplexes.

As SCR lipoplexes without galactosylation (5 mM NaCl) were intraportally injected in mice, transfection activity of SCR lipoplexes in the liver (0.39 ± 0.047 pg luciferase/mg protein) was 6-fold higher than that of conventional lipoplexes without galactosylation (0.069 ± 0.0087 pg luciferase/mg protein, $P < 0.001$ ($n = 3$)). On the other hand, transfection activity of SCR lipoplexes in the lung (0.58 ± 0.41 pg luciferase/mg protein) was slightly higher than that of conventional lipoplexes (0.34 ± 0.067 pg luciferase/mg protein, not significant); consequently the liver/lung gene expression ratio (liver selectivity index) of SCR lipoplexes without galactosylation (0.67) was 3.3-fold higher than that of conventional lipoplexes (0.20). Although enhancing effects of galactosylated SCR lipoplexes on hepatic transfection activity (20-fold increase) and liver/lung selectivity (7.8-fold increase) were more remarkable, these results of lipoplexes without galactosylation suggested that the SCR hypothesis might be commonly applicable for other gene delivery systems using liposomes.

When we injected galactosylated lipoplexes intravenously, transfection activity of galactosylated SCR lipoplexes in the liver ($9.3 \times 10^{-2} \pm 5.9 \times 10^{-2}$ pg luciferase/mg protein ($n = 3$)) was 4.1-fold higher than that of galactosylated conventional lipoplexes ($2.3 \times 10^{-2} \pm 0.7 \times 10^{-2}$ pg luciferase/mg protein ($n = 3$)). As background of tissue light emission was $0.3 \times 10^{-2} \pm 0.2 \times 10^{-2}$ pg luciferase/mg protein, intravenously administered galactosylated SCR lipoplexes exhibited hepatic transfection activity high enough to detect ($P < 0.05$), while hepatic transfection activity of galactosylated conventional lipoplexes was barely higher than the background (not significant). Therefore, liver selectivity of galactosylated SCR lipoplexes could be improved to some extent. How-

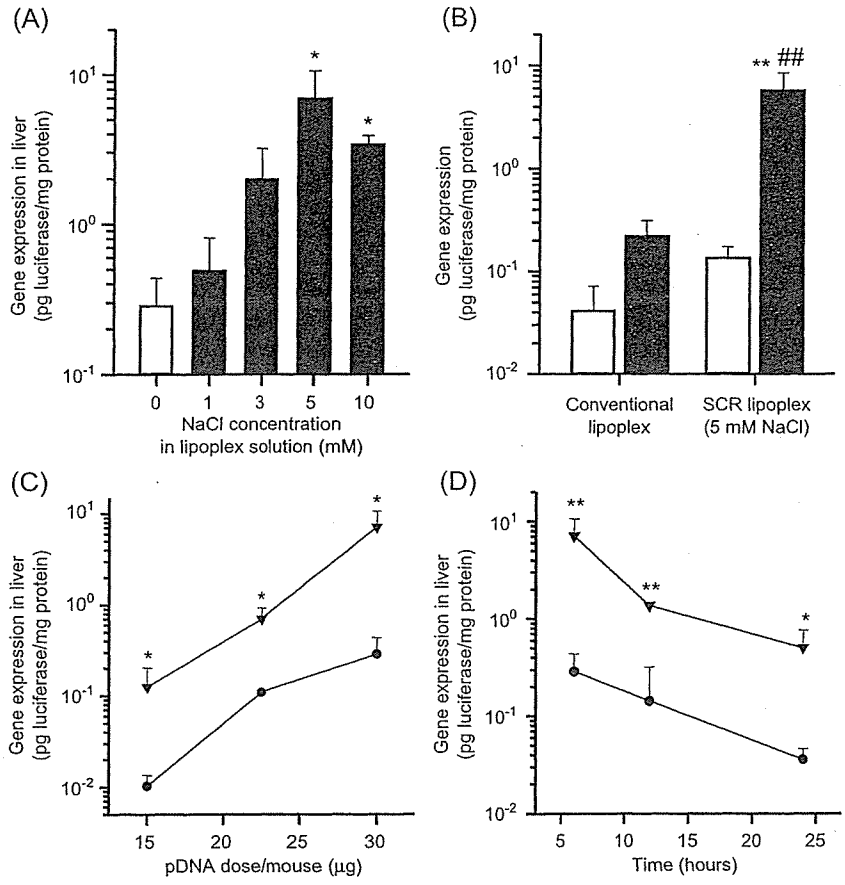

FIG. 3. Enhanced hepatic transfection activity of galactosylated SCR lipoplexes after intraportal administration in mice. Luciferase activity was determined 6 h post-injection of lipoplexes. Each value represents the mean + SD of at least three experiments. (A) Effect of NaCl concentration in the lipoplex solution on the hepatic gene transfection activity by galactosylated SCR lipoplexes. Statistical comparisons with galactosylated conventional lipoplexes were performed using Dunnett's test at a significance level of 5% (*). (B) Comparison of gene expression in liver and lung after intraportal administration of galactosylated SCR lipoplexes. Open and filled bars represent the lung and liver, respectively. Statistical comparisons were performed using Tukey's test. (** indicates comparison with galactosylated SCR lipoplexes in lung, ## indicates comparison with galactosylated conventional lipoplexes in liver: $P < 0.01$.) (C) Effect of pDNA dose on hepatic transfection activity of galactosylated SCR lipoplexes. Circles and inverted triangles represent galactosylated conventional and SCR lipoplexes (5 mM NaCl in lipoplex solution), respectively. Statistical comparisons were performed using an unpaired Student t test at each injected dose ($*P < 0.05$). (D) Duration of gene expression of galactosylated SCR lipoplexes. Circles and inverted triangles represent galactosylated conventional and SCR lipoplexes (5 mM NaCl in lipoplex solution), respectively. Statistical comparisons were performed using an unpaired Student t test at each injected dose ($*P < 0.05$, $**P < 0.01$).

ever, transfection activity of galactosylated SCR lipoplexes in the lung (1.85 ± 0.34 pg luciferase/mg protein ($n = 3$)) was also 2.6-fold higher than that of conventional lipoplex (0.72 ± 0.25 pg luciferase/mg protein ($n = 3$)). After intravenous administration, the lung gene expression was still higher than that of liver. It is well known that most of injected cationic liposome/pDNA complexes are trapped in lung capillaries during the first passage. Therefore, further studies might be needed to prevent entrapment of lipoplexes by lung for cell-selective gene delivery after intravenous administration.

In Situ Rat Liver Perfusion Evaluation of Galactosylated SCR Lipoplex

To characterize the hepatic disposition profiles of galactosylated SCR lipoplexes, we analyzed the outflow profiles in the liver perfusion experiment based on a two-compartment dispersion model [12,20]. A liver perfusion system allows us to delineate the uptake characteristics of various molecules and complexes while keeping the structure of the liver intact. Table 1 summarizes each kinetic parameter obtained from the outflow data. Assuming that lipoplexes are bound to the tissue surface and internalized (and/or sequestrated) into the liver, the k_{12}/k_{21} value represents the binding affinity for the liver tissue, while the k_{int} value represents the efficiency of internalization (and/or sequestration) of lipoplex bound to the tissue. While the forward partition coefficient (k_{12}) of the galactosylated SCR lipoplexes was similar to that of the galactosylated conventional lipoplexes, the backward partition coefficient (k_{21}) of the galactosylated SCR lipoplexes was significantly lower than that of the galactosylated conventional lipoplex. As a result, the tissue binding affinity (k_{12}/k_{21}) of the galactosylated SCR lipoplexes was 5.5-fold greater than that of the galactosylated conventional lipoplexes. The k_{int} value of the galactosylated SCR lipoplexes was comparable with that of the galactosylated conventional lipoplexes. These results suggest that the binding affinity to the liver of the galactosylated SCR lipoplexes was greatly enhanced compared with that of the galactosylated conventional lipoplexes. We investigated the hepatic cellular localization of ^{32}P-radiolabeled lipoplexes following bolus injection into perfused rat liver. When we measured the radioactivity associated with hepatocytes (liver parenchymal cells, PC) and other cells (nonparenchymal cells, NPC) per unit cell number, the PC/NPC ratio for the galactosylated SCR lipoplexes was 1.9, which was higher

doi:10.1016/j.ymthe.2004.07.015

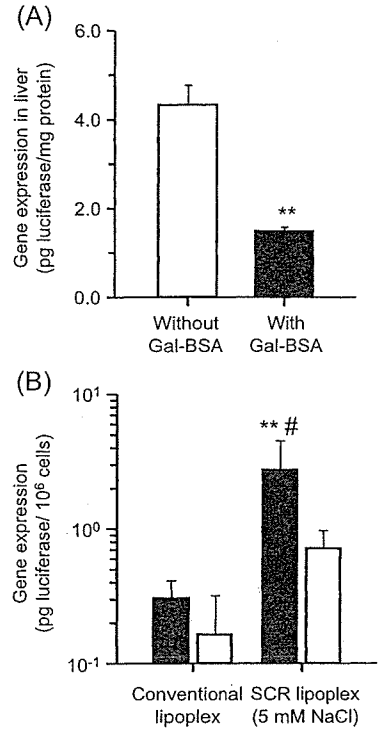

FIG. 4. Enhanced hepatocyte-selective gene transfer by galactosylated SCR lipoplexes after intraportal administration in mice. Each value represents the mean + SD of at least three experiments. (A) Inhibition of hepatic gene expression of galactosylated SCR lipoplexes (5 mM NaCl in lipoplex solution) by preadministration with or without galactosylated bovine serum albumin (Gal-BSA). Luciferase activity was determined 6 h post-injection of lipoplexes. Statistical comparisons were performed using an unpaired Student *t* test (**$P < 0.01$). (B) Intrahepatic gene expression of galactosylated SCR lipoplexes (5 mM NaCl in lipoplex solution). Luciferase activity was determined 6 h postinjection in the liver parenchymal cells (PC; filled bar) and nonparenchymal cells (NPC; open bar). Statistical comparisons were performed using Tukey's test (** indicates comparison with the PC group of galactosylated conventional lipoplexes, $P < 0.01$; # indicates comparison with the NPC group of galactosylated SCR lipoplexes, $P < 0.05$).

than that for the galactosylated conventional lipoplexes (PC/NPC ratio = 1.1) in our previous report [12]. These *in situ* experimental results partly support the belief that the *in vivo* hepatic transfection activity is enhanced by galactosylated SCR lipoplexes.

In Vitro Evaluation of Galactosylated SCR Lipoplexes

To assess whether galactosylated SCR lipoplexes exhibit superior transfection activity not only *in vivo* but also *in vitro*, we performed an *in vitro* experiment using the human hepatocarcinoma cell line HepG2, which expresses asialoglycoprotein receptors (Fig. 6). The transfection activity of the galactosylated SCR lipoplexes was significantly higher than that of the galactosylated conventional lipoplexes (Fig. 6A). In addition, these values were greatly higher than commercially available reagent Lipofectamine 2000, which enables one to transfect wide varieties of cells efficiently (0.32 ± 0.22 pg luciferase/mg protein). It is well known that pDNA released in the cytosol from the lipoplex is important for transgene expression [21–23]; therefore, we examined the intracellular localization of the galactosylated lipoplexes prepared from fluorescein-labeled pDNA and Rh-labeled liposomes by confocal laser scanning microscopy (Figs. 6B and 6C). The green, yellow, and red fluorescence indicated the emission from fluorescein–pDNA, lipoplexes, and Rh–liposomes, respectively. Rh-labeled liposomes diffused to the plasma membrane of HepG2 cells in both galactosylated SCR and conventional lipoplexes. The marked green fluorescence was more pronounced in the galactosylated SCR lipoplexes (Fig. 6C), suggesting that the galactosylated SCR lipoplexes release pDNA more easily in the cells.

DISCUSSION

Gene transfer to hepatocytes is of great therapeutic potential since hepatocytes are responsible for the synthesis of a wide variety of proteins that play important

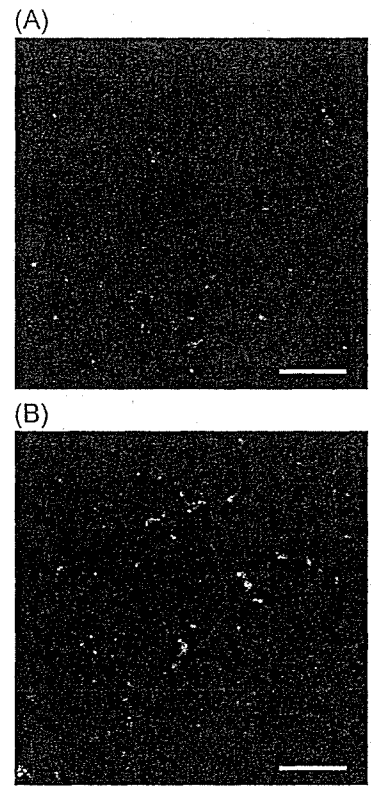

FIG. 5. Intrahepatic distribution of galactosylated (A) conventional and (B) SCR lipoplexes (5 mM NaCl in lipoplex solution) 2 h postinjection in mice. Thirty micrograms of pDNA containing 10% carboxyfluorescein-labeled pDNA complexed with galactosylated liposomes was injected intraportally. Frozen liver sections (5 μm thick) were examined by confocal laser scanning microscopy. Scale bars indicate 50 μm.

TABLE 1: Pharmacokinetic parameters of hepatic disposition of ^{32}P-labeled galactosylated SCR lipoplexes analyzed using a two-compartment dispersion model

	k_{12} (min^{-1})	k_{21} (min^{-1})	k_{12}/k_{21}	k_{int} (min^{-1})
Conventional lipoplex	30.0 ± 0.13	1.23 ± 0.23	24.9 ± 4.41	3.77 ± 0.46
SCR lipoplex (5 mM NaCl)	30.0 ± 0.08	0.22 ± 0.04[a]	136 ± 20.0[a]	3.81 ± 0.05

Results are expressed as the means ± SD of three experiments.

[a] Significant differences compared with conventional lipoplex group ($P < 0.01$).

physiological roles. There has been much interest in *in vivo* gene transfer to the liver as an alternative to *ex vivo* methods that require invasive surgery. So far, several methods involving the local administration of naked pDNA have been tested to achieve gene delivery targeted to the liver. Electroporation, the application of a controlled electric field to facilitate cell permeabilization, could enhance the transfection activity of pDNA administered via the intrahepatic, intraportal, and intravenous routes [24–26]. Similarly, instillation of pDNA onto the liver surface was recently demonstrated for liver-selective gene transfection [27]. Compared with these local applications to the liver, systemic application by vascular routes could transfect the gene to a large number of cells in the whole liver. Consequently, various nonviral vectors, including cationic liposomes and polymers, have been developed to enhance the *in vivo* gene expression. In most cases, however, the highest gene expression is observed in the lung after the intravenous administration of nonviral vectors because the lung capillaries are the first "traps" to be encountered [28,29]. In a previous study, we have demonstrated that galactosylation of the lipoplex (galactosylated conventional lipoplex) confers hepatocyte selectivity by asialoglycoprotein receptor-mediated endocytosis *in vivo* [9]. Transfection activity of galactosylated liposome complex was about 16, 22, and 50 times higher than those of naked plasmid DNA, DC–Chol liposome complex, and DOTMA–Chol liposome complex, respectively [9]. However, a number of possible barriers to a gene delivery system targeted to hepatocytes remain, e.g., (i) nonspecific interactions with erythrocytes, serum, and nontarget cells; (ii) aggregation of lipoplexes; and (iii) penetration of endothelial cells, etc., from the administration site to hepatocytes through gene expression [12,20,30–32]. Taking these into consideration, not only ligand modification (i.e., galactosylation) of the lipoplex but also controlling the stability of the ligand-modified lipoplex is important for achieving cell-selective gene transfection under *in vivo* conditions. In the present study, we demonstrated that the SCR lipoplex significantly delayed aggregation after exposure to saline compared with conventional lipoplex (Fig. 1B).

To date, lipoplexes for *in vivo* gene delivery are prepared in nonionic solution because the lipoplexes form aggregates in the presence of isotonic concentrations of ionic solutions such as saline. However, when systemically administered, the lipoplexes are exposed to the ionic solution and subsequently would aggregate as shown in the *in vitro* results (Fig. 1B). Thus, controlling the size of the lipoplex after exposure to the ionic solution is important for efficient gene delivery. We hypothesized that the presence of an essential amount of NaCl during lipoplex formation can regulate the repulsion between cationic liposomes and the fusion of the cationic liposomes in the lipoplex would be accelerated by partial neutralization of the positive charge on the surface of cationic liposomes. This hypothesis is confirmed, in part, by the results of the FRET analysis (Figs. 2A and 2B). Thus, moderate neutralization of the positive charge on the surface of cationic liposomes by a suitable concentration of NaCl can ensure sufficient repulsion of the lipoplex intermediates. However, excess neutralization of the charge by NaCl, e.g., saline (150 mM NaCl), might cause a lipoplex intermediate–intermediate interaction, followed by aggregation. The observation in the present study that the mean diameter of the lipoplex was increased by increasing NaCl concentration in lipoplex solution agrees with the recent findings by Wasan *et al.* [17]. Aggregated lipoplexes are not suitable for efficient *in vivo* hepatocyte-selective gene expression because the sinusoidal endothelium will block the penetration of such lipoplexes and, consequently, the lipoplexes would not be taken up by the hepatocytes. However, there is little concern with stabilization of lipoplex despite the fact that lipoplex aggregation must be controlled. In the present study, we demonstrated that the SCR lipoplex was shown to be relatively well protected from aggregation compared with conventional lipoplex after exposure to saline (Fig. 1B). This stabilizing effect after exposure of the SCR lipoplex to saline is also supported by the results of the FRET analysis (Fig. 2D). This effect may be partly explained by the fact that the fusion of each cationic liposome in the SCR lipoplex was enhanced (Fig. 2B); accordingly, cationic lipids may extensively cover pDNA in the SCR lipoplex. This stabilization effect on the galactosylated SCR lipoplex would be reflected in the extensive *in vivo* intrahepatic distribution after intraportal administration (Fig. 5).

To evaluate the precise hepatic uptake characteristics, a pharmacokinetic analysis for *in situ* experiments with galactosylated SCR lipoplexes was also performed. As shown in Table 1, we confirmed that the galactosylated SCR lipoplexes exhibited a higher tissue binding affinity compared with the galactosylated conventional lipo-

doi:10.1016/j.ymthe.2004.07.015

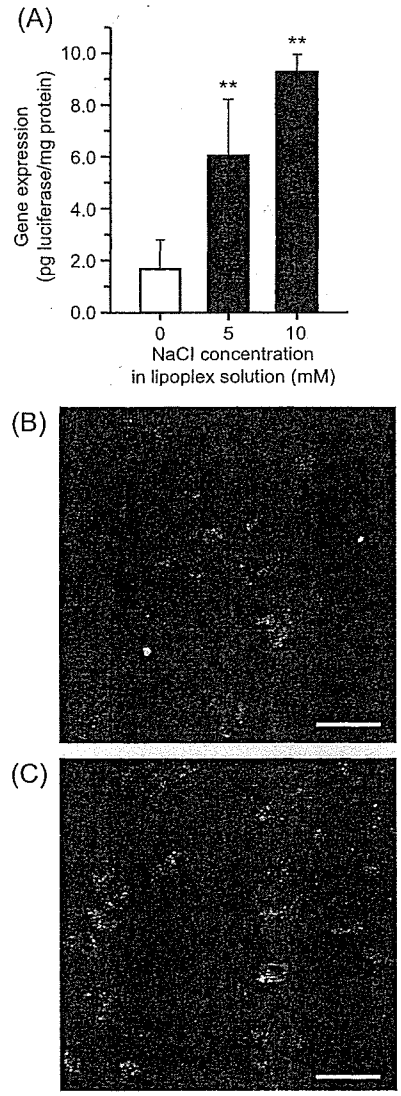

FIG. 6. (A) Transfection activity of galactosylated lipoplexes in HepG2 cells and (B, C) confocal microscopic images of galactosylated lipoplexes in HepG2 cells. (A) Luciferase activities were determined 24 h after transfection of galactosylated SCR lipoplexes. Each bar represents the mean value + SD of at least four experiments. Statistical comparisons with galactosylated conventional lipoplexes were performed using Dunnett's test at a significance level of 1% (**). (B, C) Intracellular localization of pDNA (green) and lipids (red) 4 h post-transfection of galactosylated (B) conventional and (C) SCR lipoplexes (5 mM NaCl in lipoplex solution). Scale bars indicate 50 μm. (For interpretation of the references to colour in this figure legend, the reader is referred to the web version of this article.)

plexes, while the internalization rate of the galactosylated SCR lipoplexes was similar to that of the galactosylated conventional lipoplexes. However, the amount internalized is determined by the degree of tissue binding and the internalization rate, and the total amount of the galactosylated SCR lipoplexes internalized would be increased compared with that of the conventional lipoplexes. The high tissue binding affinity and degree of internalization of the galactosylated SCR lipoplexes found in the *in situ* experiments support the results of the higher gene expression in the liver (Fig. 3) and marked intensity of the fluorescein-labeled pDNA in the liver (Fig. 5).

It has been reported that the pDNA release from the complexes in the cell is important for gene expression [21–23]. As shown in Fig. 6A, the *in vitro* transfection efficacy of the galactosylated SCR lipoplexes was significantly higher than that of the galactosylated conventional lipoplexes. To analyze the mechanism of the transfection efficacy in the cell, the intracellular localization of pDNA and lipid components was examined by confocal microscopy. Enhanced pDNA release of galactosylated SCR lipoplexes in the cells compared with galactosylated conventional lipoplexes was observed (Figs. 6B and 6C). This result may be explained by the fact that the electrostatic interaction between pDNA and the cationic liposomes in the SCR lipoplexes was reduced (Fig. 2C); consequently the weaker interaction between pDNA and the cationic liposomes led to enhanced release of pDNA in the cells. The improvements in the intracellular distribution of galactosylated SCR lipoplexes also affected the enhanced *in vivo* gene expression in the liver.

In the present study, NaCl was selected for the ionic solution to prepare the SCR lipoplexes to control the positive charge of the cationic liposomes in the lipoplex. To evaluate the possibility of using other ionic solutions for SCR lipoplex formation, we also examined the role of disodium hydrogen phosphate and sodium dihydrogen phosphate solution and found that these salts also had a similar effect on the lipoplex formation and gene expression profiles. However, the enhanced transfection efficacy produced by NaCl was higher than that by disodium hydrogen phosphate and sodium dihydrogen phosphate (data not shown). The difference between NaCl and the other salts is still unclear; but these results also provide evidence that the theory of the SCR lipoplex is available for stabilization of the lipoplex as a novel approach.

In conclusion, we demonstrated the enhanced hepatic transfection activity by stabilized galactosylated lipoplexes using sodium chloride for complex formation. FRET analysis revealed that the NaCl solution in the lipoplex weakened the repulsion among cationic liposomes and enhanced the fusion of cationic liposomes in the lipoplex; consequently, the *in vivo* transfection in hepatocytes was greatly enhanced. Pharmacokinetic studies, both *in situ* and *in vivo*, demonstrated the higher tissue binding affinity and very marked intrahepatic distribution of the galactosylated SCR lipoplex. Moreover, enhanced transfection activity of the galactosylated SCR lipoplex was observed in HepG2 cells, and the confocal microscopic images showed that the release of pDNA in the cell was greatly accelerated. These characteristics partly explain the mechanism of enhanced in vivo

transfection efficacy by galactosylated SCR lipoplex. Hence, the information we obtained will be of value for the future use, design, and development of ligand-modified lipoplexes for *in vivo* applications.

MATERIALS AND METHODS

Materials. *N*-(4-Aminobutyl) carbamic acid *tert*-butyl ester and DOTMA were obtained from Tokyo Chemical Industry Co. (Tokyo, Japan). Cholesterol was obtained from Nacalai Tesque, Inc. (Kyoto, Japan), and cholesteryl chloroformate was purchased from Sigma Chemicals, Inc. (St. Louis, MO, USA). 1,2-Dioleoyl-*sn*-glycero-3-phosphoethanolamine-*N*-(7-nitro-2-1,3-benzoxadiazol-4-yl) (NBD-DOPE) and 1,2-dioleoyl-*sn*-glycero-3-phosphoethanolamine-*N*-(lissamine rhodamine B sulfonyl) (Rh-DOPE) were purchased from Avanti Polar Lipids, Inc. (AL, USA). PicoGreen dsDNA Quantitation Reagent was purchased from Molecular Probes, Inc. (Eugene, OR, USA). [α-^{32}P]dCTP (3000 Ci/mmol) was obtained from Amersham Co. (Tokyo, Japan). Gal-BSA as a ligand of asialoglycoprotein receptors was synthesized as described in our earlier study [33]. Dulbecco's modified Eagle's minimum essential medium (DMEM) was obtained from Nissui Pharmaceutical Co. (Tokyo, Japan). Fetal bovine serum (FBS) and Lipofectamine 2000 were purchased from Invitrogen Co. (Carlsbad, CA, USA). All other chemicals were of the highest purity available.

Construction and preparation of pDNA. pCMV-Luc was constructed by subcloning the *Hin*dIII/*Xba*I firefly luciferase cDNA fragment from pGL3-control vector (Promega Co., Madison, WI, USA) into the polylinker of pcDNA3 vector (Invitrogen). pDNA was amplified in the *Escherichia coli* strain DH5α, isolated, and purified using a Qiagen Endofree Plasmid Giga Kit (Qiagen GmbH, Hilden, Germany). Purity was confirmed by 1% agarose gel electrophoresis followed by ethidium bromide staining and the pDNA concentration was measured by UV absorption at 260 nm. The pDNA for liver perfusion experiments was labeled with [α-^{32}P]dCTP by nick-translation [34]. Carboxyfluorescein labeling of pDNA for intrahepatic distribution and intracellular localization experiments was performed using the Label IT Fluorescein Nucleic Acid Labeling Kit (Mirus Co., Madison, WI, USA).

Synthesis of Gal-C4-Chol. Gal-C4-Chol was synthesized as reported previously [8]. Briefly, cholesteryl chloroformate and *N*-(4-aminobutyl)-carbamic acid *tert*-butyl ester were reacted in chloroform for 24 h at room temperature. A solution of trifluoroacetic acid and chloroform was added dropwise and the mixture was stirred for 4 h at 4°C. The solvent was evaporated to obtain *N*-(4-aminobutyl) (cholesten-5-yloxyl)formamide, which was then combined with 2-imino-2-methoxyethyl-1-thiogalactoside [35] and the mixture was stirred for 24 h at 37°C. After evaporation, the resultant material was suspended in water, dialyzed against distilled water for 48 h (12-kDa cut-off dialysis tubing), and then lyophilized.

Preparation of galactosylated cationic liposomes. Mixtures of DOTMA, Chol, and Gal-C4-Chol were dissolved in chloroform at a molar ratio of 2:1:1 for galactosylated liposomes or 1:1:0 for nongalactosylated liposomes, vacuum-desiccated, and resuspended in sterile 5% dextrose at a concentration of 4 mg total lipids per milliliter. The suspension was sonicated for 3 min and the resulting liposomes were extruded 10 times through double-stacked 100-nm polycarbonate membrane filters.

Preparation of galactosylated conventional lipoplexes and SCR lipoplexes. For galactosylated conventional lipoplex preparation, 600 μl of 200 μg/ml pDNA in 5% dextrose was mixed with an equal volume of galactosylated cationic liposomes at 1160 μg/ml and incubated for 30 min. For galactosylated SCR lipoplex preparation, part of the 5% dextrose in pDNA solution was replaced with saline and adjusted to the final NaCl concentration as indicated before being mixed with liposome solution. The mixing ratio of liposomes and pDNA was expressed as a +/− charge ratio, which is the molar ratio of cationic lipids to pDNA phosphate residue [30]. The charge ratio of unity was 2.52 μg total lipid/μg pDNA for DOTMA/Chol/Gal-C4-Chol liposomes. According to our previous report, the charge ratio was adjusted to 2.3:1.0, which exhibits the highest and most selective gene expression in the liver [9]. The particle size of the lipoplex was measured using a dynamic light scattering spectrophotometer (LS-900; Otsuka Electronics, Osaka, Japan).

FRET analysis. FRET analysis was previously applied for assessment of the stability of nonviral gene vectors by Itaka et al. [36]. Liposomes were labeled with two types of fluorescent lipid, NBD-DOPE or Rh-DOPE, at 2% (mol/mol) total lipid. pDNA was labeled with PicoGreen prior to being mixed with liposomes. The fluorescence intensity spectra were measured using a spectrofluorophotometer (RF540; Shimadzu Co., Kyoto, Japan). The excitation wavelengths were 460, 550, and 480 nm for NBD-DOPE, Rh-DOPE, and PicoGreen, respectively. The FRET from NBD–liposomes to Rh–liposomes was measured as a liposome–liposome interaction. Fusion of liposomes in the lipoplex was measured by FRET reduction caused by membrane mixing between NBD-DOPE/Rh-DOPE double-labeled liposomes and unlabeled liposomes during complex formation. FRET from PicoGreen in pDNA to Rh–liposome was measured as the pDNA–liposome interaction. FRET from NBD–lipoplex to Rh–lipoplex was measured as the lipoplex aggregation after mixing with saline.

In vivo gene expression experiments. Female 5-week-old ICR mice (20–23 g) were purchased from the Shizuoka Agricultural Cooperative Association for Laboratory Animals (Shizuoka, Japan). All animal experiments were carried out in accordance with the Principles of Laboratory Animal Care as adopted and promulgated by the U.S. National Institutes of Health and the Guidelines for Animal Experiments of Kyoto University. Mice were anesthetized by intraperitoneal administration of pentobarbital sodium (50 mg/kg). An incision was made in the abdomen, and the portal vein was exposed. pDNA complexed with cationic liposomes was administered to the portal vein (30 μg pDNA/300 μl), and the abdomen was closed by wound clips. For the *in vivo* transfection experiments, the liver and lung were excised at 6 h after injection. Each sample was homogenized with lysis buffer (0.1 M Tris/HCl containing 0.05% Triton X-100 and 2 mM EDTA (pH 7.8)). After three cycles of freezing and thawing, the homogenates were centrifuged at 10,000 *g* for 10 min at 4°C. Twenty microliters of each supernatant was mixed with 100 μl of luciferase assay solution (Picagene; Toyo Ink Mfg. Co., Tokyo, Japan) and the light produced was immediately measured using a luminometer (Lumat LB 9507; Berthold Technologies GmbH, Bad Wildbad, Germany). The gene expression is indicated as the luciferase amount per milligram of protein converted from relative number of light units using purified enzyme. The protein content of the samples was determined using a protein quantification kit (Dojindo Molecular Technologies, Inc., Gaithersburg, MD, USA). For evaluation of the intrahepatic localization of gene expression, the luciferase activities in the liver PC and NPC were independently determined after centrifugal separation of PC and NPC in collagenase-digested liver as previously described [9].

For the intrahepatic distribution study, at 2 h after injection of lipoplexes containing 10% fluorescein-labeled pDNA, the mice were killed and the livers were fixed by infusing cold 4% paraformaldehyde dissolved in PBS (pH. 7.4), followed by immersion in the fixative on ice for 2 h. The livers were subsequently embedded in Tissue-Tek OCT compound (Miles, Inc., Elkhat, IN, USA) and frozen in cold isopentane. Frozen sections, 5 μm thick, were prepared on a Cryostat (Leica Microsystems AG, Wetzlar, Germany). The liver sections were mounted on glass slides, covered by slips with 50% glycerol, and observed by confocal laser scanning microscope (MRC 1024; Bio-Rad Laboratories, Inc., Hercules, CA, USA).

Liver perfusion experiments and pharmacokinetic analysis. Male Wistar rats (170–210 g) were purchased from the Shizuoka Agricultural Cooperative Association for Laboratory Animals. *In situ* liver perfusion studies were carried out as reported previously [12,20]. Briefly, the portal vein was

doi:10.1016/j.ymthe.2004.07.015

catheterized with a polyether nylon catheter (SURFLO iv catheter, 16 G'2"; Terumo Co., Tokyo, Japan) and immediately perfused with Krebs–Ringer bicarbonate buffer supplemented with 10 mM glucose (oxygenated with 95% O_2–5% CO_2, adjusted to pH 7.4 at 37°C). The perfusate was circulated using a peristaltic pump (SJ-1211; ATTO Co., Tokyo, Japan) at a flow rate of 13 ml/min. After a stabilization period for 25 min, liposome/[^{32}P]pDNA complexes (30 μg pDNA/300 μl) were administered via the portal vein using a six-position rotary valve injector (Type 50 Teflon rotary valves; Rheodyne, Inc., Cotati, CA, USA). After addition of 5 ml Clear-Sol I, the radioactivity of the effluent perfusate was measured in a scintillation counter (LSA-500; Beckman Coulter, Inc., Fullerton, CA, USA). The outflow patterns were analyzed based on a two-compartment dispersion model involving sinusoidal and binding compartments [12,20]. The mass balance equations involving the axial dispersion in the sinusoidal space are given as

$$\frac{\partial C_S(t,z)}{\partial t} + v\frac{\partial C_S(t,z)}{\partial z} = D\frac{\partial^2 C_S(t,z)}{\partial z^2} - k_{12}C_S(t,z) + k_{21}C_B(t,z), \quad (1)$$

$$\frac{\partial C_B(t,z)}{\partial t} = \frac{1}{\varepsilon}k_{12}C_S(t,z) - k_{21}C_B(t,z) - k_{int}C_B(t,z), \quad (2)$$

where $C_S(t, z)$ and $C_B(t, z)$ are the concentrations of drug in the sinusoidal space and binding compartment, respectively; D is the dispersion coefficient; ε is the volume ratio of the binding compartment to the sinusoidal space in the liver; k_{12} and k_{21} are the forward and backward partition rate constants between the sinusoidal space and the binding compartment; k_{int} is the first-order internalization rate constant from the binding compartment to the intracellular space; v is the linear flow velocity of the perfusate; t is time; and z is the axial coordinate in the liver. The initial and boundary conditions are given as

$$C_S(t,0) = M/Q \cdot f_I(t), C_S(0,z) = 0, C_S(t,\infty) = 0, C_B(t,0) = 0, C_B(0,z) = 0,$$

where M is the amount of drug injected into the liver, Q is the flow rate of the perfusate, and $f_I(t)$ has the dimension of the reciprocal of time. Taking the Laplace transform with respect to t, rearranging, substituting the length of the sinusoidal space L with z and introducing the cross-sectional area of the sinusoidal space A, we obtain the image equation

$$\tilde{C}_s(s) = \frac{M}{Q}\tilde{f}_I(s)\cdot exp\left[\left\{\frac{Q}{2D_C} - \sqrt{\left(\frac{Q}{2D_C}\right)^2 + \frac{1}{D_C}\left\{s + k_{12} - \frac{k_{12}\cdot k_{21}}{s + k_{21} + k_{int}}\right\}}\right\}V_s\right], \quad (3)$$

where $C_s(s)$ and $f_I(s)$ denote the Laplace transform of the concentration in the venous outflow and input function $f_I(t)$, respectively. D_C is the corrected dispersion coefficient ($D_C = D \cdot A^2$), V_S is the sinusoidal volume ($= L \cdot A$), and the flow rate Q is equal to $A \cdot v$.

Each parameter (D_C, k_{12}, k_{21}, k_{int}, and V_S) was calculated by curve fitting of the Laplace-transformed equation to the experimental venous outflow pattern using a nonlinear least-squares program with a fast inverse Laplace transform algorithm, MULTI (FILT) [37]. The damping Gauss Newton method with no constraint was used for curve fitting with the MULTI algorithm. Here, $f_I(t)$ was assumed to be a δ function, since the lipoplexes were rapidly injected using a six-rotary valve injector.

For evaluation of the intrahepatic localization of uptake amounts, 30 min after injection of ^{32}P-labeled lipoplexes into the isolated perfused liver, radioactivities in the liver PC and NPC were separately determined after centrifugal separation of PC and NPC in collagenase-digested liver as previously described [9].

In vitro gene expression and intracellular localization experiments. HepG2 cells were obtained from American Type Culture Collection (Manassas, VA, USA) and maintained in DMEM supplemented with 10% FBS at 37°C under an atmosphere of 5% CO_2 in air. The cells were plated on a 12-well cluster dish at a density of 8.0×10^4 cells/3.8 cm^2 and cultivated in 1 ml DMEM supplemented with 10% FBS. All lipoplexes were prepared under the same conditions for the *in vivo* experiment to assess the mechanism of enhancing *in vivo* transfection activity of galactosylated SCR lipoplexes. For transfection experiments, the medium was replaced with 1 ml DMEM supplemented with 10% FBS containing 0.5 μg/ml pDNA complexed with liposomes after 24 h in culture. Twenty-four hours later, the cells were scraped and suspended in 200 μl PBS. Cell suspensions were subjected to luciferase assay. For intracellular localization experiments, cells were cultured on sterilized coverslips for confocal microscopy. After 24 h in culture, the medium was replaced with 1 ml DMEM supplemented with 10% FBS containing 0.5 μg/ml fluorescein-labeled pDNA complexed with Rh–liposomes. Four hours later, the cells on the coverslips were washed twice with PBS and fixed with 4% paraformaldehyde on ice for 2 h. The coverslips were mounted on glass slides with 50% glycerol and subsequently examined by confocal laser microscopy.

Statistical analysis. Statistical comparisons were performed using unpaired Student's t test for two groups (Figs. 1B, 3C, and 4A and Table 1), Tukey–Kramer's test for multiple groups (Figs. 3B and 4b) or Dunnett's test for comparison with a control group (other figures).

ACKNOWLEDGMENTS

This work was supported in part by Grants-in-Aid for Scientific Research from the Ministry of Education, Culture, Sports, Science, and Technology of Japan; by Health and Labor Sciences Research Grants for Research on Hepatitis and BSE from the Ministry of Health, Labor, and Welfare of Japan; and by the 21st Century COE Program "Knowledge Information Infrastructure for Genome Science."

RECEIVED FOR PUBLICATION JANUARY 28, 2004; ACCEPTED JULY 13, 2004.

REFERENCES

1. Smaglik, P. (2000). Gene therapy institute denies that errors led to trial death. *Nature* **403:** 820.
2. Remy, J. S., Kichler, A., Mordvinov, V., Schuber, F., and Behr, J. P. (1995). Targeted gene transfer into hepatoma cells with lipopolyamine-condensed DNA particles presenting galactose ligands: a stage toward artificial viruses. *Proc. Natl. Acad. Sci. USA* **92:** 1744–1748.
3. Ogris, M., Walker, G., Blessing, T., Kircheis, R., Wolschek, M., and Wagner, E. (2003). Tumor-targeted gene therapy: strategies for the preparation of ligand –polyethylene glycol –polyethylenimine/DNA complexes. *J. Controlled Release* **91:** 173–181.
4. Arangoa, M. A., Duzgunes, N., and Tros de Ilarduya, C. (2003). Increased receptor-mediated gene delivery to the liver by protamine-enhanced-asialofetuin-lipoplexes. *Gene Ther.* **10:** 5–14.
5. Wu, J., Nantz, M. H., and Zern, M. A. (2002). Targeting hepatocytes for drug and gene delivery: emerging novel approaches and applications. *Front. Biosci.* **7:** d717–d725.
6. Nishikawa, M., Takemura, S., Takakura, Y., and Hashida, M. (1998). Targeted delivery of plasmid DNA to hepatocytes in vivo: optimization of the pharmacokinetics of plasmid DNA/galactosylated poly(L-lysine) complexes by controlling their physicochemical properties. *J. Pharmacol. Exp. Ther.* **287:** 408–415.
7. Morimoto, K., *et al.* (2003). Molecular weight-dependent gene transfection activity of unmodified and galactosylated polyethyleneimine on hepatoma cells and mouse liver. *Mol. Ther.* **7:** 254–261.
8. Kawakami, S., Yamashita, F., Nishikawa, M., Takakura, Y., and Hashida, M. (1998). Asialoglycoprotein receptor-mediated gene transfer using novel galactosylated cationic liposomes. *Biochem. Biophys. Res. Commun.* **252:** 78–83.
9. Kawakami, S., Fumoto, S., Nishikawa, M., Yamashita, F., and Hashida, M. (2000). In vivo gene delivery to the liver using novel galactosylated cationic liposomes. *Pharm. Res.* **17:** 306–313.
10. Kawakami, S., Sato, A., Nishikawa, M., Yamashita, F., and Hashida, M. (2000). Mannose receptor-mediated gene transfer into macrophages using novel mannosylated cationic liposomes. *Gene Ther.* **7:** 292–299.

11. Kawakami, S., Yamashita, F., Nishida, K., Nakamura, J., and Hashida, M. (2002). Glycosylated cationic liposomes for cell-selective gene delivery. *Crit. Rev. Ther. Drug Carrier Syst.* **19:** 171–190.
12. Fumoto, S., Nakadori, F., Kawakami, S., Nishikawa, M., Yamashita, F., and Hashida, M. (2003). Analysis of hepatic disposition of galactosylated cationic liposome/plasmid DNA complexes in perfused rat liver. *Pharm. Res.* **20:** 1452–1459.
13. Wasan, E. K., Reimer, D. L., and Bally, M. B. (1996). Plasmid DNA is protected against ultrasonic cavitation-induced damage when complexed to cationic liposomes. *J. Pharm. Sci.* **85:** 427–433.
14. Puyal, C., Milhaud, P., Bienvenue, A., and Philippot, J. R. (1995). A new cationic liposome encapsulating genetic material: a potential delivery system for polynucleotides. *Eur. J. Biochem.* **228:** 697–703.
15. Wheeler, J. J., *et al.* (1999). Stabilized plasmid–lipid particles: construction and characterization. *Gene Ther.* **6:** 271–281.
16. Ogris, M., Steinlein, P., Kursa, M., Mechtler, K., Kircheis, R., and Wagner, E. (1998). The size of DNA/transferrin–PEI complexes is an important factor for gene expression in cultured cells. *Gene Ther.* **5:** 1425–1433.
17. Wasan, E. K., Harvie, P., Edwards, K., Karlsson, G., and Bally, M. B. (1999). A multi-step lipid mixing assay to model structural changes in cationic lipoplexes used for in vitro transfection. *Biochim. Biophys. Acta* **1461:** 27–46.
18. Gershon, H., Ghirlando, R., Guttman, S. B., and Minsky, A. (1993). Mode of formation and structural features of DNA–cationic liposome complexes used for transfection. *Biochemistry* **32:** 7143–7151.
19. Zuhorn, I. S., *et al.* (2002). Phase behavior of cationic amphiphiles and their mixtures with helper lipid influences lipoplex shape, DNA translocation, and transfection efficiency. *Biophys. J.* **83:** 2096–2108.
20. Fumoto, S., Kawakami, S., Ishizuka, M., Nishikawa, M., Yamashita, F., and Hashida, M. (2003). Analysis of hepatic disposition of native and galactosylated polyethylenimine complexed with plasmid DNA in perfused rat liver. *Drug Metab. Pharmacokinet.* **18:** 230–237.
21. Xu, Y., and Szoka, F. C. Jr., (1996). Mechanism of DNA release from cationic liposome/DNA complexes used in cell transfection. *Biochemistry* **35:** 5616–5623.
22. Koltover, I., Salditt, T., Radler, J. O., and Safinya, C. R. (1998). An inverted hexagonal phase of cationic liposome–DNA complexes related to DNA release and delivery. *Science* **281:** 78–81.
23. Sakurai, F., *et al.* (2000). Effect of DNA/liposome mixing ratio on the physicochemical characteristics, cellular uptake and intracellular trafficking of plasmid DNA/cationic liposome complexes and subsequent gene expression. *J. Controlled Release* **66:** 255–269.
24. Suzuki, T., Shin, B. C., Fujikura, K., Matsuzaki, T., and Takata, K. (1998). Direct gene transfer into rat liver cells by in vivo electroporation. *FEBS Lett.* **425:** 436–440.
25. Matsuno, Y., *et al.* (2003). Hepatocyte growth factor gene transfer into the liver via the portal vein using electroporation attenuates rat liver cirrhosis. *Gene Ther.* **10:** 1559–1566.
26. Liu, F., and Huang, L. (2002). Electric gene transfer to the liver following systemic administration of plasmid DNA. *Gene Ther.* **9:** 1116–1119.
27. Kawakami, S., *et al.* (2002). Liver- and lobe-selective gene transfection following the instillation of plasmid DNA to the liver surface in mice. *Biochem. Biophys. Res. Commun.* **294:** 46–50.
28. Li, S., and Huang, L. (1997). In vivo gene transfer via intravenous administration of cationic lipid–protamine–DNA (LPD) complexes. *Gene Ther.* **4:** 891–900.
29. Mahato, R. I., Takakura, Y., and Hashida, M. (1997). Nonviral vectors for in vivo gene delivery: physicochemical and pharmacokinetic considerations. *Crit. Rev. Ther. Drug Carrier Syst.* **14:** 133–172.
30. Yang, J. P., and Huang, L. (1997). Overcoming the inhibitory effect of serum on lipofection by increasing the charge ratio of cationic liposome to DNA. *Gene Ther.* **4:** 950–960.
31. Li, S., Tseng, W. C., Stolz, D. B., Wu, S. P., Watkins, S. C., and Huang, L. (1999). Dynamic changes in the characteristics of cationic lipidic vectors after exposure to mouse serum: implications for intravenous lipofection. *Gene Ther.* **6:** 585–594.
32. Sakurai, F., *et al.* (2001). Interaction between DNA and–cationic liposome complexes and erythrocytes is an important factor in systemic gene transfer via the intravenous route in mice: the role of the neutral helper lipid. *Gene Ther.* **8:** 677–686.
33. Nishikawa, M., Miyazaki, C., Yamashita, F., Takakura, Y., and Hashida, M. (1995). Galactosylated proteins are recognized by the liver according to the surface density of galactose moieties. *Am. J. Physiol.* **268:** G849–G856.
34. Sambrook, J., and Maniatis, T. (1989). Molecular Cloning: A Laboratory Manual, Second ed. Cold Spring Harbor Laboratory Press, Plainview, NY.
35. Lee, Y. C., Stowell, C. P., and Krantz, M. J. (1976). 2-Imino-2-methoxyethyl 1-thioglycosides: new reagents for attaching sugars to proteins. *Biochemistry* **15:** 3956–3963.
36. Itaka, K., Harada, A., Nakamura, K., and Kataoka, K. (2002). Evaluation by fluorescence resonance energy transfer of the stability of nonviral gene delivery vectors under physiological conditions. *Biomacromolecules* **3:** 841–845.
37. Yano, Y., and Tanaka, H. (1989). A nonlinear least squares program, MULTI (FILT), based on fast inverse Laplace transform for microcomputers. *Chem. Pharm. Bull.* **37:** 1035–1038.

Available online at www.sciencedirect.com
SCIENCE DIRECT
Journal of Controlled Release 98 (2004) 157–167
journal of controlled release
www.elsevier.com/locate/jconrel
GENE DELIVERY

Tissue and intrahepatic distribution and subcellular localization of a mannosylated lipoplex after intravenous administration in mice

Makiko Yamada, Makiya Nishikawa, Shigeru Kawakami, Yoshiyuki Hattori, Takayuki Nakano, Fumiyoshi Yamashita, Mitsuru Hashida*

Department of Drug Delivery Research, Graduate School of Pharmaceutical Sciences, Kyoto University, Sakyo, Kyoto 606-8501, Japan

Received 4 December 2003; accepted 19 March 2004

Abstract

We have previously reported that, unlike a lipoplex and mannosylated (Man) lipoplex underwent gene transfer to liver nonparenchymal cells (NPC) that possess mannose receptors after intravenous administration in mice. In this study, the tissue, intrahepatic distribution, and subcellular localization of the lipoplex after intravenous administration were investigated. DC-Chol liposome was selected as a cationic liposomes. After administration of lipoplex and Man lipoplex, the high gene expression was observed in the lung and liver, respectively. After administration of [^{32}P]Man lipoplex, about 80% of [^{32}P]plasmid DNA (pDNA) was accumulated in the liver. As for the intrahepatic distribution, the NPC/parenchymal cells (PC) ratio of [^{32}P]Man lipoplex was 9.64, whereas the NPC/PC ratio of [^{32}P]lipoplex was 1.93. The radioactivity in the cytosolic fraction of liver homogenate of [^{111}In]Man lipoplex was two-fold higher than that of [^{111}In]lipoplex, indicating that Man liposomes facilitate the release of pDNA into the cytosolic space. However, a rapid sorting of the radioactivity from endosomes to lysosomes was observed with the [^{111}In]Man lipoplex. Also, amplification of pDNA by PCR suggested that the Man lipoplex is more rapidly degraded within the intracellular vesicles than the lipoplex. These results suggested that modulation of its intracellular sorting could improve the transfection efficiency of Man lipoplex.

Keywords: Gene delivery; Mannose receptor; Mannosylated liposomes; Cationic liposomes; Plasmid DNA

1. Introduction

The success of in vivo gene therapy relies on the development of a vector that achieves target cell-specific, efficient, and prolonged transgene expression following its application. Nonviral vectors are considered to be less toxic, less immunogenic, and easier to prepare than viral vectors and are, therefore, attractive vectors for clinical application. One of the most promising class of nonviral vectors developed so far is the cationic liposome-based transfection system. The lipoplex formation via electrostatic interaction of cationic liposomes and plasmid DNA (pDNA) facilitates the interaction of pDNA with cell membranes, leading to transgene expression in the cells [1]. In an attempt to increase the efficiency of transgene expression as well as to reduce cytotox-

* Corresponding author. Tel.: +81-75-753-4525; fax: +81-75-753-4575.
E-mail address: hashidam@pharm.kyoto-u.ac.jp (M. Hashida).

0168-3659/$ - see front matter © 2004 Elsevier B.V. All rights reserved.
doi:10.1016/j.jconrel.2004.03.021

icity, several kinds of cationic lipids, such as quaternary ammonium detergents, cationic derivatives of cholesterol [2], diacylglycerol [1,3], and alkyl derivative of polyamines [4] have been developed. Among them, some lipoplex have been used in clinical trials for the treatment of cancer and cystic fibrosis [5,6].

The lipoplex is a useful nonviral vector, but it lacks specificity in delivery and transfection after systemic administration. Although the levels of gene expression vary from study to study, the lung invariably shows the highest gene expression. The attachment of a ligand that can be recognized by a specific mechanism would endow a vector with the ability to target a specific population of cells. In the search for macromolecule-based nonviral vectors, several ligands including galactose [7,8], mannose [9,10], transferrin [11], and antibodies [12] have been used to improve the delivery of pDNA to target cells. Therefore, the incorporation of such ligands into cationic liposomes would improve the cell specificity of in vivo gene transfer by lipoplex.

Mannose receptor-mediated targeting is a promising approach to achieve cell-specific delivery after systemic administration because (i) the expression of mannose receptors is restricted to the liver NPC and other macrophages, (ii) a complex entering the systemic circulation has easy access to the liver NPC, and (iii) the liver has a high blood flow. These physical and biological features give a mannosylated vector an opportunity to deliver pDNA to the liver NPC via mannose receptor-mediated endocytosis. Liver nonparenchymal cells (NPC), including sinusoidal endothelial cells and Kupffer cells, can be the targets for gene therapy because they have been implicated in a wide variety of diseases [13,14].

In a previous study, we developed a novel mannosylated derivative of cholesterol, cholesten-5-yloxy-*N*-(4-((1-imino-2-D-thiomannosylethyl)amino) butyl)formamide (Man-C4-Chol), and used it to prepare a cationic liposome formulation (Man liposome) [10]. Man-C4-Chol possesses multi-functional properties, that is, (i) a lipophilic anchor moiety (cholesterol) for stable incorporation into liposomes, (ii) a mannose moiety for recognition by the mannose receptors, and (iii) an imino group for binding to pDNA via electrostatic interaction [15]. Furthermore, low-molecular-weight glycolipids are more promising due to their low immunogenicity, high reproducibility, and ease of mass production. Although, a high gene expression in the liver and spleen after intravenous injection was observed for Man lipoplex via mannose receptor-mediated endocytosis compared with the lung, its transfection efficiency was relatively low and, consequently, further improvements in the efficiency of transgene expression are required.

In order to obtain a theoretical strategy to develop an efficiently targetable gene carrier to the liver by mannosylation, therefore, detailed information on the distribution of a Man lipoplex needs to be obtained. In the present study, we studied the tissue, intrahepatic distribution, and subcellular localization of a [^{32}P]- or [^{111}In]-labeled Man lipoplex after intravenous administration. The results were compared with those for a 3β[*N*′,*N*′,*N*′-dimethylaminoethane]-carbamoyl]cholesterol liposomes (DC liposome), which is a cationic cholesterol derivative, based lipoplex [2].

2. Materials and methods

2.1. Chemicals

N-(4-Aminobutyl)carbamic acid *tert*-butyl ester was purchased from Tokyo Chemical Industry (Tokyo, Japan). Cholesteryl chloroformate was obtained from Sigma (St. Louis, MO, USA), dioleoylphosphatidylethanolamine (DOPE) was purchased from Avanti Polar-Lipids (Alabaster, AL, USA). [α-^{32}P]dCTP was obtained from Amersham (Tokyo, Japan). ^{111}Indium chloride ([^{111}In]$InCl_3$) was supplied by Nihon Medi-Physics (Hyogo, Japan). Diethylenetriaminepentaacetic acid (DTPA) anhydride and 4-[*p*-azidosalicylamido]butylamine (ASBA) were purchased from Dojindo (Kumamoto, Japan) and Pierce Biotechnology (Rockford, IL, USA). Man-C4-Chol [10] and DC-Chol [2] were synthesized as reported previously. Mannosylated bovine serum albumin (Man-BSA) was synthesized and radiolabeled with [^{111}In]$InCl_3$ as reported previously [16]. All other chemicals were obtained commercially as reagent-grade products.

2.2. Construction and preparation of pDNA

pCMV-Luc was constructed by subcloning the *Hin*dIII/*Xba*I firefly luciferase cDNA fragment from

pGL3-control vector (Promega, Madison, WI, USA) into the polylinker of pcDNA3 vector (Invitrogen, Carlsbad, CA, USA). pDNA was amplified in the E coli strain DH5α, isolated, and purified using a QIAGEN Endofree Plasmid Giga Kit (QIAGEN, Hilden, Germany). Purity was confirmed by 1% (w/v) agarose gel electrophoresis followed by ethidium bromide staining and the DNA concentration was measured by UV absorption at 260 nm.

2.3. Animals

Female ICR mice (5-week-old, 20–25 g) were obtained from the Shizuoka Agricultural Co-operative Association for Laboratory Animals (Shizuoka, Japan). All animal experiments were carried out in accordance with the Principles of Laboratory Animal Care as adopted and promulgated by the US National Institutes of Health and with the Guidelines for Animal Experiments of Kyoto University.

2.4. Preparation of liposomes

Man-C4-Chol (8.1 μmol) or DC-Chol (10.0 μmol) was mixed with DOPE (5.4 μmol for Man-C4-Chol and 6.7 μmol for DC-Chol) in chloroform (5.0 ml) and evaporated to dryness in a round-bottomed flask. Then, the lipid film was vacuum desiccated to remove any residual organic solvent and resuspended in 5% (w/v) dextrose (2.5 ml). After hydration, the dispersion was sonicated for 5–10 min in a bath sonicator to produce liposomes. The liposome formulations were passed through a polycarbonate membrane filter (0.22 μm) for sterilization. The liposomal lipid concentration was determined by phosphorous analysis [17] and was adjusted to 3 mg/ml.

2.5. Lipoplex formation

The mixing ratio of liposomes with pDNA was expressed as a charge ratio, which is the molar ratio of the cationic lipids to the pDNA phosphate residues [18]. The charge ratio (+: −) of these liposomes and pDNA complex was adjusted to 2.3:1.0 for cell-selective gene transfection [19,20]. A solution of cationic liposomes (0.2 ml) was added to an equal volume of pDNA solution (0.2 ml and pDNA concentration ≅0.33 μg/μl) in a polyethylene tube. Then, the lipoplex was agitated rapidly by pipetting it up and down twice using a micropipette (PIPETMAN®, GILSON, Villier-le Bel, France) and left to stand for 30 min. The particle size and zeta potential of the lipoplex were measured using a dynamic light scattering spectrophotometer (LS-900, Otsuka Electronics, Osaka, Japan) and a laser electrophoresis zeta-potential analyzer (LEZA-500T, Otsuka Electronics), respectively.

2.6. pDNA radiolabeling methods

pDNA was radiolabeled with [α-^{32}P]dCTP by nick translation [21]. In a separate preparation, pDNA was radiolabeled with ^{111}In using a newly developed method [22]. Briefly, a dimethylsulfoxide solution of ASBA was added to DTPA anhydride under darkroom conditions, and the mixture was incubated at room temperature for 1 h. Then, pDNA solution was added to the mixture, and the mixture was immediately irradiated under an UV lamp at room temperature for 15 min to obtain DTPA-ASBA coupled pDNA (DTPA-ASBA-pDNA). The product was purified by precipitation twice with ethanol, and labeled with [^{111}In]$InCl_3$. The purity of each pDNA was checked by Sephadex G-25 column chromatography and 1% (w/v) agarose gel electrophoresis.

2.7. Gene expression experiments

Five-week-old ICR mice were injected intravenously with 300 μl of lipoplex using a 30-gauge syringe needle. Three or six hours after injection, mice were killed and lung, liver, kidney, spleen, and heart were removed and assayed for gene expression. The organs were washed twice with cold saline and homogenized with lysis buffer (0.05% Triton X-100, 2 mM EDTA, 0.1 M Tris, pH 7.8). The lysis buffer was added in a weight ratio of 5 μl/mg for liver samples or 4 μl/mg for other organ samples. After three cycles of freezing and thawing, the homogenates were centrifuged at 10,000 × g for 10 min at 4 °C and 20 μl supernatant was analyzed to determine the luciferase activity using a luminometer (Lumat LB9507, EG and G Berthold, Bad Wildbad, Germany). The protein